AUTOMATED IDENTIFICATION OF TRAFFIC DETECTOR MALFUNCTIONS

By Katherine R. Riffle

A Thesis

Submitted in Partial Fulfillment

of the Requirements for the Degree of

Master of Science

in Civil Engineering

Northern Arizona University

December 2021

Approved:

Edward Smaglik, Ph.D., P.E., Chair

Brendan Russo, Ph.D., P.E.

Steven Gehrke, Ph.D.

1.0   PREFACE AND INTRODUCTION

The included manuscript chapters were created for the SPR837 project with Oregon DOT. Some redundancy will result from combining these articles within the Northern Arizona University formatting requirements, as both articles have foundations in the same fundamental traffic theories.

The purpose of the first article's research is to use manual drone video data alongside fundamental traffic theories to evaluate vehicle detector performance. The detectors that pass this heuristic evaluation are then used in the second article's research. The purpose of the second article's research is to provide guidance for the action and implementation of detector health analysis as a low-cost option for updating faulty infrastructure. The algorithm developed for this end is described in the second article.

I thank Professor Smaglik for managing this research and guiding this thesis. I thank Professor Russo and Professor Gehrke for their statistical guidance.

2.0   LITERATURE REVIEW

The objective of this literature review is to explore previous research relevant to the areas of detector performance, detector health monitoring, and traffic flow theory as it applies to detector operations.

2.1 DETECTION TECHNOLOGY

Outside of downtown grid networks, signalized intersections are typically operated with some type of actuation. The complexity of the actuated control algorithm is directly related to the vehicle detection required to effectively operate the control. With control algorithms ranging from legacy call and extend operation to complex traffic responsive and adaptive operations, detection requirements can vary from as simple as a presence detection zone to call a side street phase for service to an array of sensors covering a network tasked with delivering presence, count, and occupancy information.

Vehicle detection falls into two general categories, invasive technologies, those which are within the pavement, and non-invasive technologies, located outside of the roadway surface. Invasive sensors are commonly based upon inductive detection, taking the form of an in-pavement wire loop, preformed loop, small form factor loop (micro-loop), or wireless magnetometer. Non-invasive sensors vary in technology, including video, both visible and infrared, radar, and recently to the market, combination video and radar units. In-pavement wired loops have been deployed in vehicle sensing operations for fifty years, with wireless magnetometer units entering

the marketplace a little more than a decade ago. Various non-invasive sources have been

employed in assorted vehicle detection operations for more than twenty years. It is noted that,

per the direction of the Technical Advisory Committee (TAC), inductive loop and radar

technologies will be used to develop the algorithms in this work; as such, little focus will be

given to other detection sources.

2.1.1 INDUCTIVE LOOP DETECTOR

Historically, inductive loop detection has been the most widely used sensor for vehicle detection

(Day et al. 2011) and, when functioning properly, have been purported to be the most accurate

detection technology available. Loop detectors are installed in the pavement at various points

leading up to an intersection. Figure 2-1 shows an example schematic of a typical loop
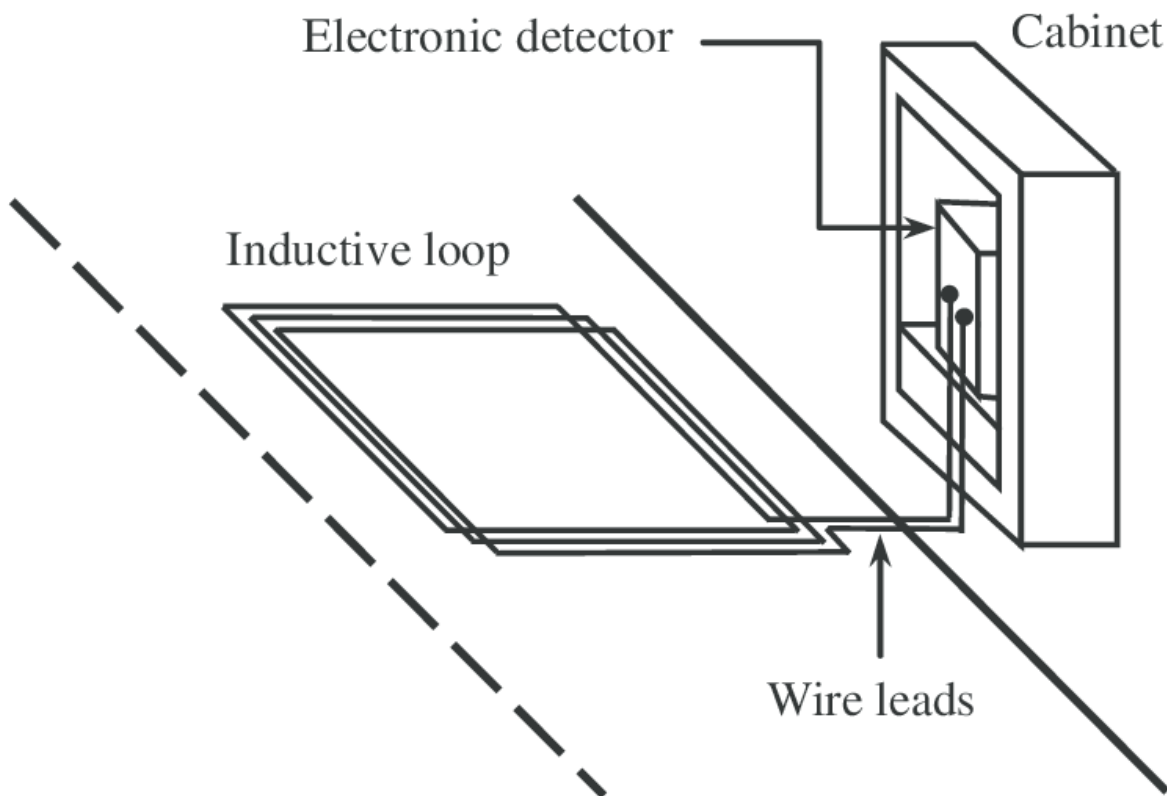
installation.

Figure 2-1: Wire Inductive Loop Setup (Lamas et al. 2016)

Inductive loop detection has been used as a ground truth in a number of other detection

performance evaluations (Christopher Day et al. 2010) (Rhodes, Bullock, and Sturdevant 2006)

(Grossman et al. 2012), and using the performance characteristics of an inductive loop, the

Indiana Department of Transportation (INDOT) developed detection performance specification

(INDOT 2015) (Middleton et al. 2009) to address the issue of detector latency and other

performance issues identified with non-invasive detection devices. Inductive loops are not

without their challenges, however. Placing loops directly into the pavement can exacerbate

pavement distress. While preformed loops placed under the surface course do not have this

drawback, both types of installations are susceptible being compromised due to common in-

ground hazards, including freeze/thaw cycling, vermin, and wayward construction equipment, all of which can cause performance degradation and impact detector health.

2.1.2 RADAR DETECTION

Radar technology has been in use for the development of vehicle performance measures on freeway facilities for a number of years, however only recently have products been brought to market to employ this technology at signalized intersections. Earlier units focused on advance detection only, avoiding the inherent challenge of detection vehicles at the stop line with a technology that uses object motion to operate. Researchers at the Texas A&M Transportation Institute (TTI) tested a unit in 2008 and found that the unit accounted for a 23-48% increase in phase termination over video detection (Middleton, Charara, and Longmire 2009). Research personnel at Purdue University noted that the use of this type of technology for advance detection has the potential to increase both efficiency and safety of dilemma zone protection since it tracks the vehicle all the way through the detection zone as opposed to extrapolating from an advance speed trap (Sharma et al. 2008). These results were supported by (Hurwitz et al. 2012) who documented a reduced frequency of drivers captured in the type two dilemma zone when a wide area radar detection system was employed as compared to in-pavement loops. Another research group noted that the units recorded speed and volume values comparable to loops during both free flow and congested conditions, although some occlusion issues were noted (Minge, Kotzenmacher, and Peterson 2010). In favorable weather conditions, false and missed calls ranged from 0.4% to 6.1% of vehicles. Investigation into the performance of these units under varying environmental conditions has been conducted, with the researchers noting

that an increase in precipitation was correlated to performance degradation (Medina, Ramezani, and Benekohal 2013). Performance degradation for radar units can also come from out-of-date software, movement of the unit so that it no longer is pointing at the proper target area, and failure of the individual radio channels inside the unit.

Figure 2-2 shows a radar set up on a pole at an intersection in Florida from the brand Wavetronix. Radar detectors are most commonly positioned at a high elevation to provide a wide, unobstructed view of the intersection to minimize issues with occlusion.

Figure 2-2: Wavetronix Radar Detector (Huotari 2015)

2.2 DETECTOR HEALTH MONITORING

Monitoring of detector health can be generally divided into three separate methods: monitoring through traffic control products, monitoring through traffic control software / algorithm, and monitoring through the use of in-person assessments. The following subsections will detail what is available in scientific as well as vendor literature regarding these techniques.

2.2.1 DETECTOR HEALTH MONITORING WITH TRAFFIC CONTROL PRODUCTS AND SOFTWARE

As was noted earlier, most traffic controllers and detection devices are able to detect major detector failures by examining the presence, absence, or frequency of data being sent by a detector, but these tools are not able to assess the quality of the information sent; therefore, the health of the detector is commonly unmonitored. For example, detrimental detector behaviors at signalized intersections such as a loop that fails for 3 minutes and works for 1 minute may not send a phase into recall, and therefore may not be observed.

Given the implementation of Q-Free/Intelight products on the ODOT system, the research team reached out to the vendor to request information regarding how their products monitor detector health ("MAXVIEW Atms" 2020). The email response from Patrick Marnell, a project manager at Q-Free, is included in Appendix A (Marnell 2020), and summarized as follows:

MAXTIME local control software includes three ways to identify a malfunctioning sensor. Collectively these features are called "detector diagnostics" in the software. These are an optional feature that can be programmed per detector.

- No Activity – Assume a failure if no calls are received on a detector for a configurable period of time.
- Max Presence – Assume a failure if a continuous call is placed on a detector for a configurable period of time.
- Erratic Count – Assume a failure if a more than a specified number of calls are placed on a detector in a configurable period of time.

When a detector is considered failed, a couple responses are possible.

- Place a minimum or maximum recall.
  - MAXTIME software is pretty flexible on this and lets you pick between Min 1 or Min 2 and Max 1, Max 2, or Max 3.
- Define a "failed link" detector.
  - This defines a detector that will be used in lieu of inputs from a failed detector.

The controller has some internal storage where detector failures will be logged for a limited period of time. If a jurisdiction is using MAXVIEW atms (central system) then they can also get alarms pulled into a Traffic Management Center type program for review.

As noted from this communication, MAXVIEW does identify detector faults, but only at the ends of the performance spectrum. If performance has degraded slightly due to increased latency or some other performance issue, this would likely not be identified.

Other vendors incorporate similar capabilities in their control software. Econolite's Centracs SPM central system specifications notes that this system applies statistical data science to analyze detectors that may not be fully operational, and creates a list within the monitored corridor that may have degraded detector performance (Econolite 2020b). To accomplish this, Econolite's traffic controller can be programmed to identify a lack of activity on a certain detector by time of day as a possible failure. Additionally, their SPM tool can look historically at previous days to identify differences and use that information to flag a failure.

McCain is another manufacturer that sells controllers and intersection control software, but their published literature does not detail how their products address sensor health (McCain 2020), and attempts to acquire further information from the manufacturer were unsuccessful.

In researching detector health monitoring accomplished by detection devices, the research team reviewed various inductive loop and radar detection units and noted that the extent of health monitoring is reporting faults and logging them. Vendor websites did not provide detail on how faults were identified, however given what is known about common practices by the research team, it is presumed that faults are identified by examining the presence, absence, or frequency of data being sent by a detector. (Econolite 2020a; Iteris 2020; Reno A&E 2020; "Wavetronix - SmartSensor V" 2020)

2.2.2 DETECTOR HEALTH MONITORING THROUGH ALGORITHMS / POST PROCESSING

Algorithms can be used either in real time or through post-processing to identify problematic detector operation. Statistical methods can be used to identify outliers, infeasible data, and erroneous data, making it suitable to develop graphs and tables to find the location of the erroneous data within the data set. From there, it is possible to find the detector itself that was causing the poor data quality. While the work in this project is focused on interrupted flow facilities, algorithms in applied to uninterrupted flow are considered as well.

Researchers at the Washington State Transportation Center developed an algorithm to identify and correct dual-loop sensitivity problems that resulted in inaccurate reporting of truck volumes. Using individual vehicle information developed from event based high resolution data, the researchers were able to identify sensitivity discrepancies and then retune the detectors, the end result of this work being the implementation of the algorithm in a software tool for convenient usage (Nihan, Wang, and Cheevarunothai 2006). In a study that used loop detector data from almost 15,000 Caltrans inductive loops, malfunctioning loops are identified through their volume and occupancy measurements. These measurements are compared against values at neighboring detectors as well as historical data to identify when a detector may be problematic, improving on earlier methods that only relied on data from a single detector (Chen et al. 2003). In related work, researchers at the University of Nebraska developed a methodology to identify malfunctions such as detector and communication failures that lead to erroneous data (Vanajakshi and Rilett 2006). This research focused on the conservation of vehicles principle on

11

a system-wide level to identify locations where the principle was violated. It was then validated

using a CORSIM model.

The Portland Oregon Regional Transportation Archive Listing (PORTAL) is the ITS data

archive for freeway loop detector data for the Portland metropolitan region, documenting

aggregated data and performance measures. Data uploaded into PORTAL is filtered to identify

erroneous data through a series of data quality flags as well as comparison against plausibility

thresholds. For the former technique, if a detector logs a speed as zero when the same detector

logs a count greater than zero, a flag is raised. For the latter technique, data samples that have a

speed about 100 miles per hour, or below five miles per hour would be flagged. Data samples

are then broken into four categories: Good, Suspicious (failed one or more data quality

conditions), No Traffic, or Communication Failure. This information is then made known to the

user when downloaded and can also be plotted to identify the scale of erroneous data by type of

filter. Figure 2-3 shows a monthly report that is used to compare data samples from detectors to

find failing units based on occupancy, volume, and speed thresholds (Tufte et al. 2007).
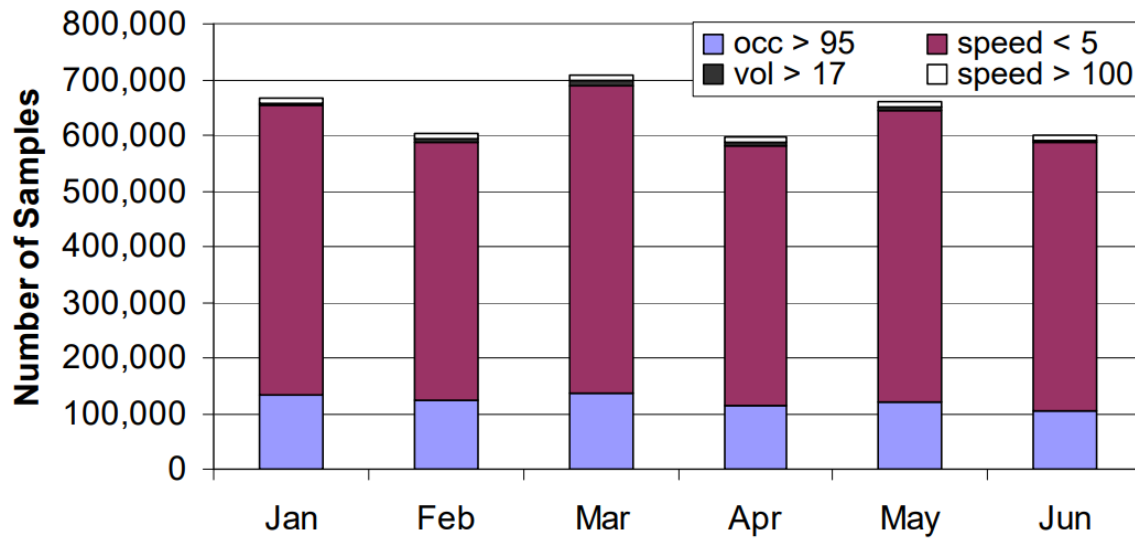
Figure 2-3: PORTAL - Number of Samples Failing Selected Conditions (Tufte et al. 2007)

Researchers in Sweden and Finland collaborated to develop a Fuzzy Intelligent Traffic Signal (FITS) control, a method which provides an inexpensive approach to improve signal control based on road infrastructure (J Jin et al. 2016). A simulation-based framework is used to evaluate different traffic control strategies based on certain criteria such as vehicle flows, pedestrian flows, priorities, and platoon management. In this methodology, stop line detectors assist in vehicle actuated timing and advance detectors play a crucial role in the decision making process (J Jin et al. 2016). In running their FITS simulations, the researchers determined that traffic states can still be properly estimated and proper decisions can be made even if a few detectors are malfunctioning, though the authors noted that there is a threshold where this falls apart (J Jin et al. 2016). Another project that related detection performance to advanced signal control was commissioned by Oregon DOT and completed in 2017. In this project, researchers at Northern Arizona University led a team that investigated the impact on non-invasive detection

13

performance on adaptive control. As part of their site evaluation researchers noted that only 42% of the coupled detection zones (inductive loop and non-invasive technology) passed a human ground truth comparison. Additionally, the research team was able to identify other poorly performing detectors by comparing collected detector data (for example, occupancy with a video detector) with expected performance norms. One of the conclusions of this study was that detector health monitoring is critical for sensors used for higher level control (Smaglik et al., 2017).

In a recent study, a screening tool was developed to identify detector errors from data within the Utah DOT detector data database. This work used statistical analysis as well as historical detector information to identify malfunctioning detectors from data within the database through a multi-stage process, using a combination of historical data, data from neighboring detectors, and the application of traffic flow theory to detector data to identify problematic detectors. Data was compiled from UDOT's Performance Measurement System (PeMS) from detectors along a corridor. The PeMS system received vehicle count and occupancy data at 20 second intervals. Speed, flow, and occupancy were analyzed to find potential errors in a one-month data collection period. The primary method of detector health evaluation in this study was through comparison of adjacent detectors upstream or downstream of each other on this roadway. (TRB 2020)

2.2.2.1   Automated Traffic Signal Performance Measures (ATSPMs)

ATSPMs started in the mid-2000s with the collection and analysis of high-resolution event based data for traffic signal performance (Smaglik et al., 2007). Since then, researchers at Purdue

University along with practitioners at the Indiana Department of Transportation and Utah

Department of Transportation have evolved the use of event based data into a method of

assessing and improving the performance of traffic signals, traffic signal systems, and traffic

signal system business practices (Day et al., 2014). From a technical standpoint, the suite of

ATSPMs can allow an agency to monitor capacity, progression, multimodal, and maintenance

performance measures without the added expense of a central- or adaptive traffic signal system.

These performance measures can be developed though robust communication and typical traffic

signal detector information, though additional detection is required to take advantage of all the

performance measures. On the topic of detection performance, detector health can be

determined through identification of phases in recall over time, as this is an indication that the

detector is not performing properly. These locations are aggregated and then reported to agency

managers for repair prioritization.

2.2.3 DETECTOR HEALTH MONITORING THROUGH ON-SITE INVESTIGATION

While it is preferable to identify malfunctioning detectors through off-site means, equipment and

procedures can be implemented on-site as well. Researchers in Germany developed a portable

Malfunction Sniffer to identify errors in inductive loop detector outputs (Kuhnel, Weisheit, and

Hoyer 2011). Their device, shown in Figure 2-4, was effectively a portable method of ground

truthing detector data. Once programmed with the exact location of the detection zones, the

system would corroborate the outputs of the detectors with an audiovisual signal indicating

vehicle passage so that supervisor could monitor the output. It was noted that this system did not work as well for video detectors.
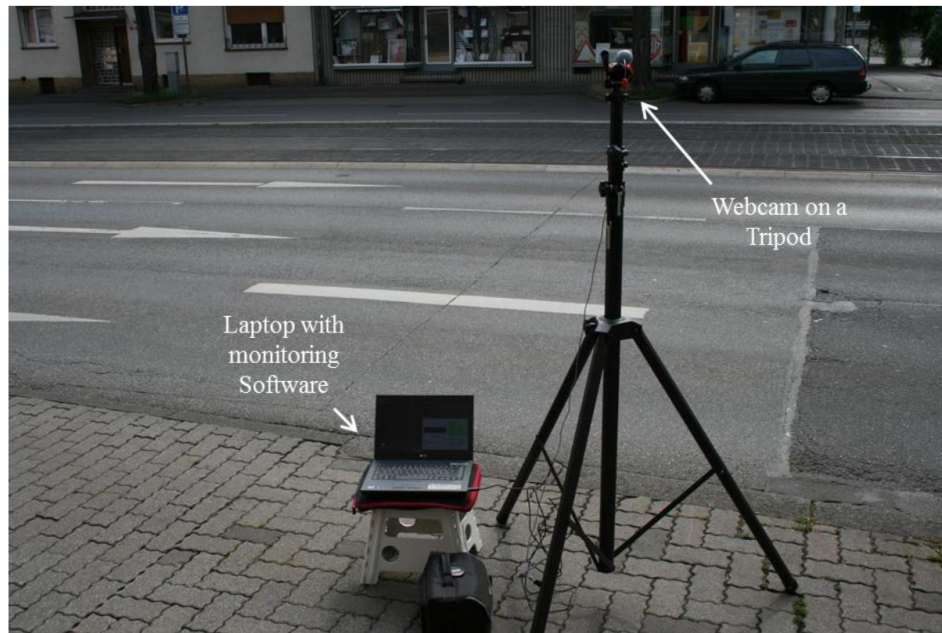

Figure 2-4: Malfunction Sniffer (Kuhnel, Weisheit, and Hoyer 2011)

A project sponsored by the Federal Highway Administration (FHWA) attempted to use Ground Penetrating Radar (GPR) to identify the location of loop detectors, determine if they were functioning, and perform detailed analysis to assess the conditions of the sensor (Arnold et al. 2011). While the device developed and deployed in this work was able to accomplish all three goals to some degree, it was noted that the device was not able to detect defect and deterioration, and further work is required. Lastly, in a study performed by Purdue University, wireless magnetometers were tested against a standard loop detector to evaluate their effectiveness and accuracy at picking up calls. While wireless magnetometers are not the focus of this work, one conclusion of this study was that 8 foot spacing be observed between sensors adjacent to the stop

line to minimize missed calls, indicating that design standards may have an impact on the performance of detection devices (C Day et al. 2010).

2.3 TRAFFIC FLOW THEORY AND FUNDAMENTAL WORK

2.3.1 GREENSHIELDS MODEL

Traffic flow theory is the basis of conceptual modeling of traffic. Greenshields Model of traffic flow (Greenshields 1935) is an elegant relationship that illustrates the connected nature of volume, speed, and density within traffic operations. This relationship, shown in Equation 1, leads to the fundamental diagrams of the Greenshields model, shown in Figure 2-5.
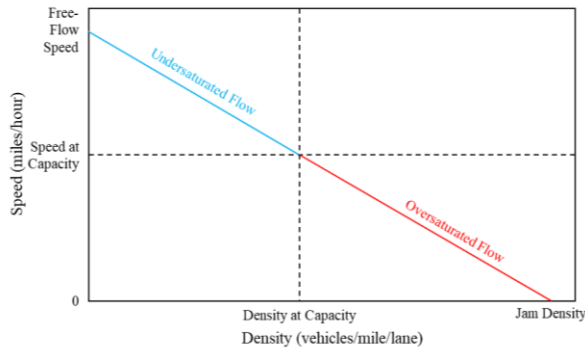
$$V = S * D \qquad \textbf{Equation 1}$$
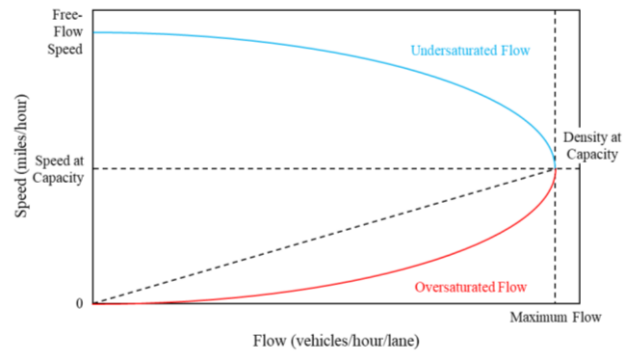
Where: **V = Volume (vehicles/hour)**
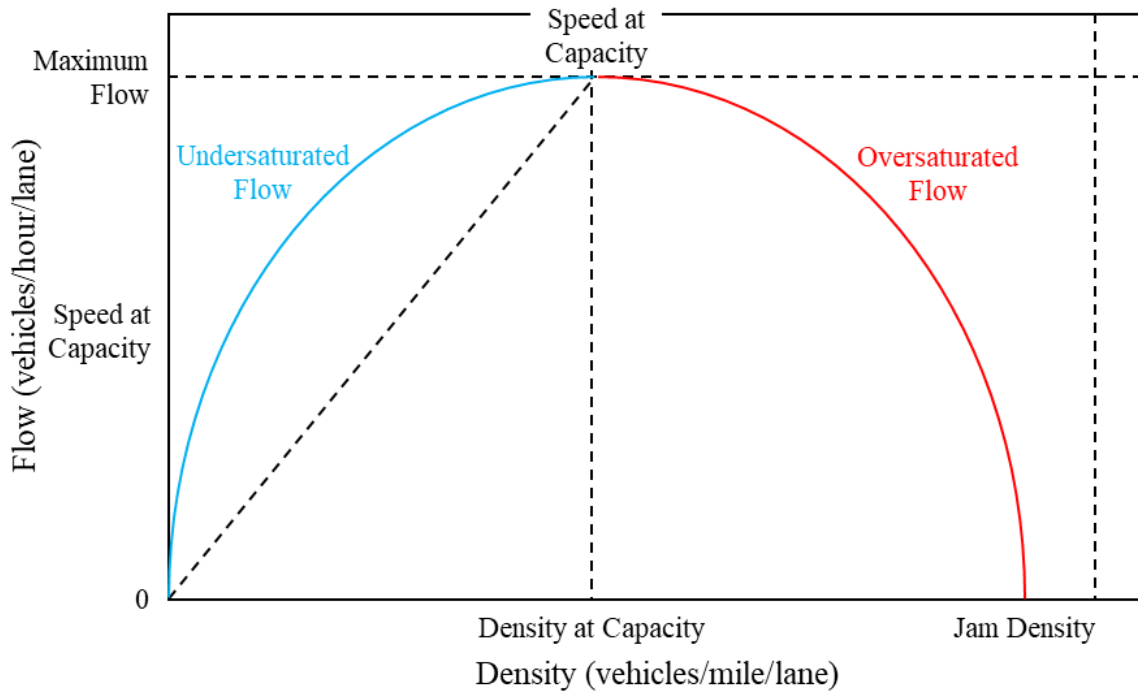
S = Speed (miles/hour)

D = Density (vehicles/mile)

(a) Speed vs Density

(b) Speed vs Flow (Volume)

(c) Flow (Volume) vs Density

Figure 2-5: Fundamental Diagrams of Greenshields Model: (a) Speed vs Density; (b) Speed vs Flow (Volume); (c) Flow (Volume) vs Density

These diagrams illustrate the idealized conceptual relationships between the three macroscopic traffic stream parameters, volume, speed, and density. They encompass two distinct regions of flow, undersaturated (under capacity) and oversaturated (over capacity). These diagrams are

conceptual in nature, in that volume, speed, and density data collected to model traffic flow at any given location when plotted would not give way to a smooth diagram as is shown in Fig. 8, but would look more like Figure 2-6, which is a Speed / Density plot developed from real world data. The linear dashed line in Figure 2-6 represents Greenshields model, while the red points are the empirical data.
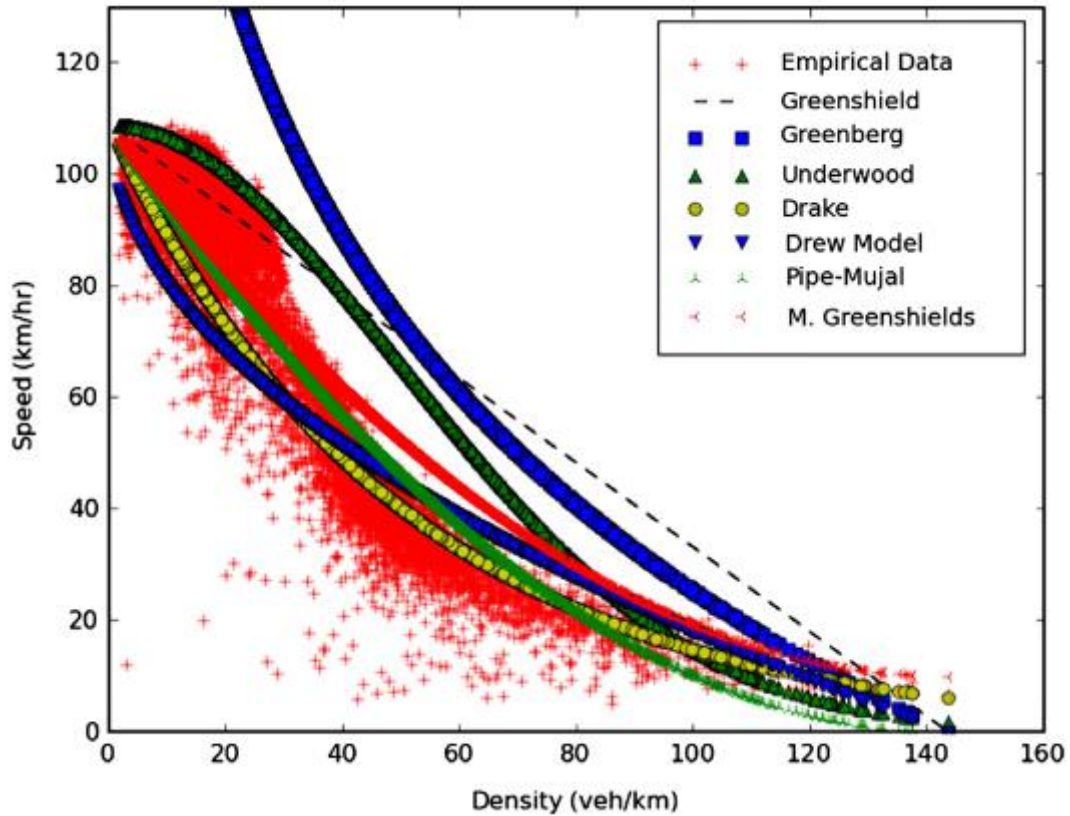

Figure 2-6: Real world Speed-Density plot (Wang et al. 2011)

The fundamental diagrams have been used in traffic research to assist in the investigation of incident detection (Jing Jin and Ran 2009), car-following models for simulation (Deng and Zhang 2012), the effects of weather on traffic operations (Dhaliwal et al. 2017), and variable speed limits (Bertini, Boice, and Bogenberger 2006), among countless other topics, but to the research team's knowledge have not been used in detector health applications.

19

2.3.2 SATURATED FLOW RATE AND HEADWAYS

The departing vehicle flow rate at capacity from a signalized intersection is defined as the

Saturation Flow Rate. This rate of flow occurs as vehicles in a standing queue depart, starting

from the 5th vehicle in the queue as the first four vehicles in the queue depart at a lower flow rate

due to time lost as the queue moves from a stopped to a moving queue (Transportation Research

Board 2016). This Saturation Flow Rate can be determined in three separate ways. First, it can

be calculated based upon site characteristics using methods set forth in the Highway Capacity

Manual, as shown in Figure 2-7.

$$s = s_0\, f_w\, f_{HVg}\, f_p\, f_{bb}\, f_a\, f_{LU}\, f_{LT}\, f_{RT}\, f_{Lpb}\, f_{Rpb}\, f_{wz}\, f_{ms}\, f_{sp}$$

where

s = adjusted saturation flow rate (veh/h/ln),

s_o = base saturation flow rate (pc/h/ln),

f_w = adjustment factor for lane width,

f_{HVg} = adjustment factor for heavy vehicles and grade,

f_p = adjustment factor for existence of a parking lane and parking activity adjacent to lane group,

f_{bb} = adjustment factor for blocking effect of local buses that stop within intersection area,

f_a = adjustment factor for area type,

f_{LU} = adjustment factor for lane utilization,

f_{LT} = adjustment factor for left-turn vehicle presence in a lane group,

f_{RT} = adjustment factor for right-turn vehicle presence in a lane group,

f_{Lpb} = pedestrian adjustment factor for left-turn groups,

f_{Rpb} = pedestrian–bicycle adjustment factor for right-turn groups,

f_{wz} = adjustment factor for work zone presence at the intersection,

f_{ms} = adjustment factor for downstream lane blockage, and

f_{sp} = adjustment factor for sustained spillback.

Figure 2-7: Calculation of Saturation Flow Rate (Transportation Research Board 2016)

Second, it can be directly measured in the field by counting the vehicles departing at capacity during a certain time period. Lastly, it can be determined in the field by measuring departure headways of vehicles departing at capacity, with headway defined as, "the time between successive vehicles as they pass a point on a lane or roadway, measured from the same point on each vehicle" (Transportation Research Board 2016). The relation between headway and volume is shown in Equation 2. If the headway measured occurs during queue discharge at capacity, the corresponding volume that will be calculated will be that of the saturation flow rate.

$$V = \frac{3600}{h} \qquad \textbf{Equation 2}$$

Where: **V = Volume (vehicles/hour)**

                               h = Departure headway (seconds/vehicle)

The concepts of headway, saturation headway, and saturation flow rate were developed through applied research, and as part of the foundation of traffic operations theory, appear in research endeavors covering all aspects of traffic theory, including intersection capacity (Laufer et al. 2019), the impact of automated vehicles on mixed-use lanes (Mohajerpoor and Ramezani 2019), bicycle operations (Raksuntorn and Khan 2003), geometric design (Potts et al. 2007), and weather conditions (Asamer and Van Zuylen 2011), among others, but they have not been applied to detector health.

2.4 CONCLUDING REMARKS

This literature review has covered the basics of inductive loop and radar detection technology, the state of the practice regarding detector health monitoring, and the elements of traffic theory that will be used in monitoring detector health. Inductive loops, when functioning properly, are purported to be the most accurate detection technology, likely due to their close proximity to the traffic being detected, a consequence of being an invasive technology. But, because of their invasive nature, there are a number of issues that can compromise the performance of an inductive loop detection. Radar detection, one type of non-invasive detection, has been shown in research to be generally reliable, with environmental factors causing a minimal impact on performance, however internal components can fail without a complete failure of the unit, which can also compromise performance.

In the area of detector health, three different techniques were covered in this literature review: monitoring with traffic control products and software, monitoring with algorithms / post processing, and on-site monitoring. Traffic control products and software typically identify poorly performing detectors through monitoring for flickering, lack of a call, or a constant call from a specific detector. Most online vendor literature is vague when it comes to describing how detector health is monitored, if mentioned at all. This, combined with the lack of information in the literature focused on detector health monitoring in the field, indicates that detector health monitoring is typically accomplished with these aforementioned heuristics. If data is post processed, a number of different methods can be used to identify problems with detector health. This can be accomplished through comparing detector outputs with outputs of neighboring detectors, comparing detector outputs with historical data, or evaluating detector data with

plausibility thresholds. Additionally, using ATSPMs, the health of a detector is monitored by identifying actuated phases operating in recall, an indication that the detector is not providing proper information to the controller. Lastly, on-site investigations can also be conducted to identify poorly performing detectors, if so desired.

Finally, Greenshields model and content within the Highway Capacity Manual form the theoretical basis for capacity analysis of interrupted and uninterrupted flow facilities. Each intersection approach has a unique discharge capacity that can be either calculated or measured in the field through two separate methods. These methods, along with the fundamental diagrams yielded through application of Greenshields' model, and combined with high resolution detection data, reveal an opportunity to monitor detector health through traffic flow information on a per intersection approach basis.

This thesis contributes to the existing literature in two ways: First, by introducing a new process of manually verifying vehicle detectors, and second, by developing new algorithms for detector monitoring. Regarding the former, the process of using drone video to record and transcribe data for individual vehicles over detection zones is specifically useful in research endeavors. Maneuvering one set of devices to record minimal video data for multiple vehicle detectors and intersections is useful for collecting very accurate data for these detectors. It is preferable to installing new cameras for research purposes, because it costs less and can retrieve videos at specific angles more appropriate for identifying vehicles entering and exiting detection zones. Regarding the latter, the algorithms subsequently developed in this thesis contribute methods of detector health analysis to the literature. Existing methods do not use Greenshields models and theories of traffic flow to analyze individual detectors at signalized intersections. Automated methods of detector monitoring are important to allow more wide-spread and efficient detector

malfunction identification in state DOTs. The developed algorithms introduce metrics for detector health evaluation applicable to detectors with event-based data outputs.

The remainder of this thesis report is structured as follows. Chapter 3 includes the manuscripts that were submitted to tier-one peer-reviewed journals; the first manuscript was limited to 2500 words, and the second manuscript was limited by number of pages. Chapter 4 will then explore the conclusions, lessons learned, and limitations of this project.

3.0   MANUSCRIPT CHAPTERS

A Novel Method of Detector Performance Verification

Katherine Riffle, Yujun Liu, Eileen Chai, David Hurwitz, Ph.D, Edward Smaglik,

Ph.D., and Brendan Russo, Ph.D.

Past research [1] has shown declining operational performance of vehicle detectors over time at signalized intersections. This study uses statistical methods to compare event-based data from vehicle detectors to manually transcribed drone video data to identify malfunctioning loop and radar detectors, and can be used in further research to verify detector performance at intersections without existing video cameras.

Background

Unmonitored declining vehicle detector performance reduces intersection safety and efficiency. This study develops a novel method of detector performance verification by using collected and transcribed drone video data and comparing it to detector event log data. Existing literature has limited information on detector health monitoring in the field, indicating that detector health monitoring is accomplished primarily by checking for complete failure (always on, always off, or flickering) [2] [3] [4] [5]. Using post-processed data, additional methods of identifying detector health problems include comparing detector outputs with outputs of neighboring detectors, comparing detector outputs with historical data, or evaluating detector data with plausibility thresholds [6] [7] [8]. Automated Traffic Signal Performance Measures can assess detector performance by monitoring actuated phases operating in recall indicating that the detector is not providing proper information to the controller [9] [10]. While the above methods are useful for assessing detector performance across a network, some quality of assessment is lost due to the lack of video surveillance. Previous studies have used existing video cameras to provide a higher

quality assessment of detector performance through manual verification and transcription [1]. The same level of assessment was required for the detection areas in this work, as they were to be used to develop an algorithm to monitor detector health over time, presuming they were healthy. However, with no cameras onsite, drones were used as part of an analysis process that included drone video collection, data transcription, and comparison to event log detector outputs through two statistical methods. Drone video recordings were higher quality and provided preferable overhead viewing angles than post-mounted intersection cameras otherwise would have.

Drone Video Collection

Six study sites in Oregon were surveyed with a drone to inventory existing infrastructure elements as well as record video of vehicles passing over detection zones. Specific researcher roles and responsibilities were established to ensure safe and efficient field data collection: Remote Pilot-in-Command (PIC), Visual Observer (VO), and Research Assistants. This experiment required the use of a drone, a high-resolution camera, a landing pad, a solar powered electric generator, and a distance measuring wheel. A DJI Mavic 2 Pro was used to collect all drone data in the field. The landing pad made it easier to initiate takeoffs and landings on uneven terrain, the field generator was used to recharge drone batteries in the field between flights, the measuring wheel was used to document the dimensions of detectors and their distance from the stop lines, and personal protective equipment (PPE) contributed to the safety of researchers in the field. Before the field work could be performed, Oregon State University (OSU) fulfilled nine Oregon Department of Transportation (ODOT) Unmanned Aircraft System Contractor Requirements to ensure compliance with local regulations in addition to those stipulated by the Federal Aviation Administration.

Detector Position and Dimensions

Graduate Research Assistants used signal plans provided by ODOT, photographs collected on site, and distance measuring wheels to confirm the existence, placement, and dimensions of detectors. These details were annotated on field photographs and signal plans. Figure 1 shows an example of road measurement details. A research assistant measured the diameter of the circular detectors, the nearest length from detector to stop line (placement), and the dimensions of the parallelogram detectors.
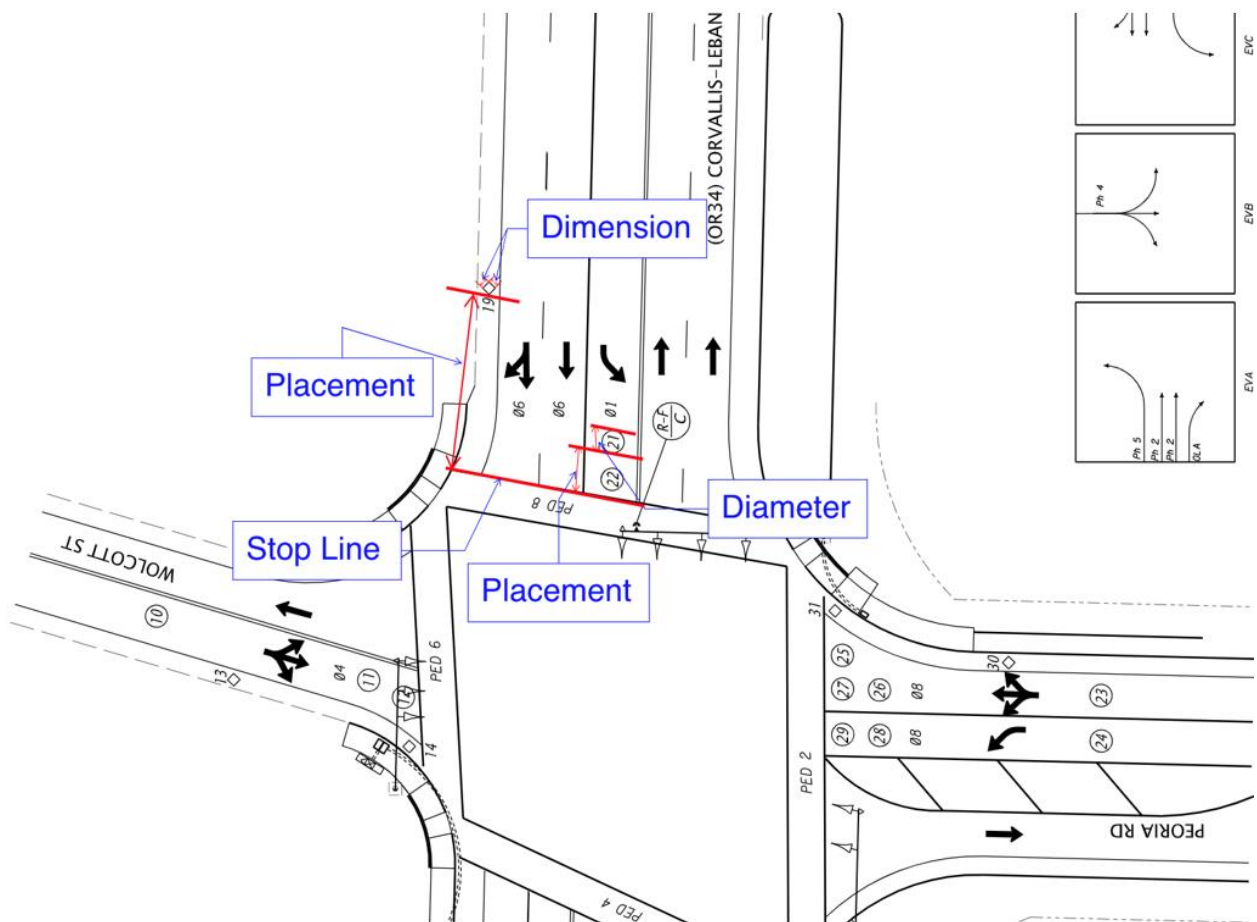
Figure 1: Road Measurement Details

Drone Video of Vehicles Driving over Detectors

This work surveyed six sites in total, each with a number of in-pavement loop or radar detectors. Table 1 provides information about the drone video data collected from the detectors, including the dates that the drone video data was collected on. It also indicates the numbers of each detector classified as a stop line detector or advanced detector; with a detector considered to be stop bar detector if it is 75 feet or closer to the stop line on the subject approach.

Table 1: Drone Video Data Collected

Site	Type		Location		Date
	Loop	Radar	Stop Line	Advanced	
OR22 @ I-5 SB Offramp	12	0	2	10	Nov 7 2020
OR34 @ I-5 SB Ramp	5	9	7	7	Nov 8 2020
OR34 @ Peoria	14	0	5	9	Oct 31 2020
US20 @ 15th	12	0	4	8	Nov 8 2020, Nov 21 2020
US26 @ Meinig-Pioneer	10	0	5	5	Dec 5 2020
US101 @ 22nd	17	0	9	8	Nov 21 2020

Each of the six selected signalized intersections has a unique detector configuration. To collect usable videos (i.e. stable images with good contrast of detectors against pavement) the weather conditions and the drone position were carefully considered. Additionally, some detectors were located hundreds of feet away from each other. These factors required multiple drone flights on each approach to directly observe each detector. With one available drone and nine batteries, the video observations were collected one intersection per day and one video at a time with a maximum video duration of approximately 20 minutes.

To ensure the safety of the drone, the research team, and the traveling public, as well as to ensure the quality of videos, research assistants found an appropriate area to set up the landing pad. This was a critical choice in avoiding collisions with power lines, span wires, tree branches, and other overhead obstacles. Once the drone was in flight, as stipulated by the Federal Aviation Administration, the maximum flight elevation could not exceed 400 feet, and the drone must not fly over the road or any non-research personnel. Moreover, the VO needed to continuously survey the surrounding environment while the PIC adjusted the camera angle to ensure the detectors and traffic signal display were captured on video simultaneously. During the recording period, the PIC was responsible for attending to the drone and the controller, maintaining constant communication with the VO, and ensuring the flight occurred safely until the drone landed. After the field data was collected, research assistants cropped the videos, added timestamps, and transcribed the video data.

Drone Video Data Transcription

The video captured by the drone was transcribed to obtain usable ground truth information about detector calls. As vehicles traversed an active detection zone, time stamps were recorded when the front bumper of the vehicle arrived at the upstream edge of the highlighted circular loop detector zone (Figure 2a) and again when the rear bumper of the vehicle departed the downstream edge of the detector zone (Figure 2b). Additionally, the active traffic signal display was recorded during each call for service. Transcription for an individual detection zone was performed for either the duration of the entire video or for the first 100 vehicle incursions.

(a) call on   (b) call off

Figure 2: Detector 19 on the NB approach of US20 and 15th Street

Event Log Data

The drone videos were compared to processed event-based detector output logs, which report

information using Event IDs and corresponding Parameters [9]. The list of used Event IDs and the

corresponding Parameters are shown in Table 2. Event IDs 1 and 8 were used to identify the

starting timestamps of each green and yellow phase, to determine the length of each cycle and

each green and yellow/red phase. Event IDs 82 and 81 indicated *Vehicle Detector On* and

Vehicle Detector Off, respectively. With all radar and loop detection zones operating in presence,

data from these events can be used to determine activations (a surrogate for vehicle counts in this

work, as count detector outputs are not available).

Table 2: Event Log IDs and Parameters [9]

Event ID	Name	Description	Parameter Description
1	Phase Begin Green	Set when either solid or flashing green indication has begun	Phase #
8	Phase Begin Yellow Clearance	Set when phase yellow indication becomes active and clearance timer begins	Phase #
81	Vehicle Detector Off	Vehicle detector has turned off. Detector on and off events are triggered post any detector delay/extension processing	Vehicle Detector #
82	Vehicle Detector On	Vehicle detector has turned on. Detector on and off events are triggered post any detector delay/extension processing	Vehicle Detector #

Two of the sites provided for this work are equipped with radar detection, in addition to inductive loop detection. Only radar count zones operating in 'Normal' mode (akin to a loop detector operating in presence mode) were used in this analysis, as the outputs of the larger stop line and advance radar detection zones are manipulated by proprietary vendor software to achieve various objectives, and as such, their outputs will vary from what one might be able to visually observe through vehicle interactions.

Event Log Data Reduction and Preparation

While the timestamps on the drone Video Log were close to the timestamps in the Event, the specific Event Log data which corresponded directly to the reduced drone video data needed to be identified. Specific individual vehicles were identified within both data sets, and the time between *Vehicle Detector On* indications in both the Video Log and Event Log were used to match a specific Event Log vehicle activation with the corresponding Video Log vehicle activation. This process was conducted for the first and last vehicle of each Video Data log to develop a complete list of Event Log *Vehicle Detector On* and *Vehicle Detector Off* activations

corresponding to activity in the Video Log during that timeframe. Then, the initial vehicle green indication noted in the Video Log was used to shift the timestamps so that the initial vehicle activation in both the Video Log and Event Log occurred simultaneously. Next, the number of activations and duration of each activation was determined from both data sets. This process was undertaken for each detection zone with available data. An example of the activation duration data reduction is shown in Table 3.

Table 3: Timestamps Example: Detector On and Off Indications for Detector 7 OR22 at I-5

Detector Indication (minutes:seconds.00)				Detector On Duration	
Video Log		Event Log		Video Log	Event Log
On	Off	On	Off	= Off - On	= Off - On
43:29.67	43:31.13	43:30.10	43:31.70	0:00:01.46	0:00:01.60
43:32.13	43:33.27	43:32.60	43:33.80	0:00:01.14	0:00:01.20
43:37.80	43:38.67	43:38.20	43:39.10	0:00:00.87	0:00:00.90
43:44.37	43:44.90	43:44.90	43:45.40	0:00:00.53	0:00:00.50
43:46.53	43:47.10	43:47.00	43:47.60	0:00:00.57	0:00:00.60
43:59.33	43:59.90	43:59.70	44:00.40	0:00:00.57	0:00:00.70
44:07.23	44:08.40	44:07.80	44:09.00	0:00:01.17	0:00:01.20
44:12.43	45:24.77	44:12.90	45:25.40	0:01:12.34	0:01:12.50
45:28.30	45:29.60	45:28.80	45:30.30	0:00:01.30	0:00:01.50
45:31.00	45:32.23	45:31.70	45:32.80	0:00:01.23	0:00:01.10
45:34.87	45:36.03	45:35.50	45:36.70	0:00:01.16	0:00:01.20
45:47.63	45:47.93	45:48.20	45:48.50	0:00:00.30	0:00:00.30

Finally, it should be noted that for radar count detection zones, the Event Log outputs were compared to the Video Log for closest neighboring inductive loop detector for activation counts only, as the exact location of the radar count zone is not visible. For the advanced detectors that span the width of the entire approach, the activations of multiple neighboring loop detectors were compiled chronologically to develop a consistent comparative set.

Detector Performance Evaluation Comparative Metrics

With the datasets prepared as in Table 3, two separate metrics for comparative analysis of the two logs were used to determine whether or not the detector would be considered 'healthy'. The first comparative metric used was the total number of activations noted by each log during the analysis period. A difference threshold of 10%, as calculated by Equation 2, determined whether or not the detector was healthy regarding activations. The 10% threshold is a rule of thumb used when comparing counts from vehicle sources, and has been previously used in research for detector performance [1] [10].

Equation 2: Activation Difference Calculation

$$\frac{Total\ Observation\ Event\ Log\ Activations - Total\ Observation\ Video\ Log\ Activations}{Total\ Observation\ Video\ Log\ Observations}$$

The second metric for evaluating detector health was the *Detector On Duration*. When combined with an analysis of period duration, this metric can determine the occupancy of a detection zone. As shown in Table 4, the *Detector On Duration* was found for each activation for both the Event Log and Video Log datasets. The distributions of *Detector On Durations* for both the Video Log and Event Log were compared using a paired t-test to identify statistically significant differences (an f-test was used to check whether each pair of distributions had equal or unequal variances, and the corresponding t-test was used based upon the outcome of that test). If the t-test indicated a significant difference, then the detector was determined to be unhealthy for the purpose of this analysis [11].

Results

Table 4 shows the results of the *Detector On Duration* t-tests and the *Number of Activations* comparisons for the detectors at one intersection , indicating which detectors passed the comparative analyses. A similar table was created for each detector in the study, indicating whether the detector passed both evaluation metrics.

Table 4: t-test Outputs for OR22 @ I-5

Det	Activations				Detector On Duration Mean			Passed Both Comparisons
	Manual	Event Log	Difference	% Diff	Manual	Event Log	Difference	
1	100	95	-5	-5.0%	00:00.3	00:00.4	00:00.0	Y
2	105	103	-2	-1.9%	00:00.3	00:00.4	00:00.0	Y
3	72	72	0	0.0%	00:00.3	00:00.3	00:00.05**	N
4-6	100	90	-10	-10.0%	00:00.4	00:00.5	00:00.1	Y
7	58	58	0	0.0%	00:03.7	00:03.7	00:00.0	Y
8	75	75	0	0.0%	00:02.4	00:02.6	00:00.2	Y
9-10	103	98	-5	-4.9%	00:03.8	00:04.9	00:01.1	Y
11-12	59	76	17	28.8% *	00:09.4	00:08.0	-00:01.40	N
13-14	78	59	-19	-24.4% *	00:07.8	00:09.3	00:01.6	N
15	100	48	-52	-52.0% *	00:00.2	00:00.6	00:00.34**	N
16	100	58	-42	-42.0% *	00:00.3	00:00.9	00:00.59**	N
17-18	100	93	-7	-7.0%	00:01.0	00:01.0	00:00.1	Y
* indicates a difference of >10% between the Manually reported and Event Log number of activations								
** indicates Significant Difference at 95% CI in the Detector On Durations as reported by the t-Test								

In this work, a total of 79 detection zones underwent the comparative analyses (70 inductive loop and 9 radar). Of the inductive loop detection zones, 39 passed the analysis, while 6 of the radar zones passed the analysis, for a total of 45 valid detection zones, ~60% of the total analyzed.

Concluding Remarks

This study developed and tested a novel method of detector health evaluation by statistically comparing manually collected and transcribed drone video data to event-based detector output logs. The process of using drone video to record and transcribe data for individual vehicles over detection zones has a specific place in research and practice, when a high-fidelity assessment of detector performance needs to be conducted at a location without existing video surveillance. Maneuvering one set of drone devices to record short-term video data for multiple vehicle detectors and intersections is useful for collecting very accurate data for these detectors. It is preferable to installing new cameras for research purposes and for practice in circumstances requiring highly accurate video information, as it costs less and videos can be retrieved at specific angles more appropriate for identifying vehicles entering and exiting detection zones.

Acknowledgments/Disclaimer

References

[1] Smaglik, C Sobie, A Sharma, C Liu, and S Kothuri. 2017. "Improving Adaptive/Responsive Signal Control Performance: Implications of Non-Invasive Detection and Legacy Timing Practices." Final Report FHWA-OR-RD-17-07. Oregon.

[2] Econolite. 2020a. "AccuSense Control - Econolite Radar Vehicle Detection." Econolite (blog). 2020. https://www.econolite.com/products/detection/accusense-control/.

[3] Iteris. 2020. "Iteris Vantage Vector." May 2020. https://www.iteris.com/products/detection-sensors/vantage-vector-hybrid.

[4] Reno A&E. 2020. "Reno A&E Vehicle Detectors." May 2020. http://www.renoae.com/Category/root/30.

[5] "Wavetronix - SmartSensor V." 2020. 2020. https://www.wavetronix.com

[6] Chen, C, J Kwon, J Rice, A Skabardonis, and P Varaiya. 2003. "Detecting Errors and Imputing Missing Data for Single Loop Surveillance Systems." In , 25 p. Washington DC, United States.

[7] Tufte, K, S Ahn, R Bertini, B Auffray, and J Rucker. 2007. "Toward Systematic Improvement of Data Quality in Portland, Oregon, Regional Transportation Archive Listing." In , 11 p. Washington DC, United States: Transportation Research Board.

[8] Vanajakshi, L, and L Rilett. 2006. "System-Wide Data Quality Control of Inductive Loop Data Using Nonlinear Optimization." Journal of Computing in Civil Engineering 20 (3): pp 187-196.

[9] Day, Christopher, Darcy Bullock, Howell Li, Steve Remias, Alexander Hainen, Richard Freije, Amanda Stevens, James Sturdevant, and Thomas Brennan. 2014. "Performance Measures for Traffic Signal Systems: An Outcome-Oriented Approach." JTRP Affiliated Reports, August. https://doi.org/10.5703/1288284315333.

[10] Smaglik, Edward J., Anuj Sharma, Darcy M. Bullock, James R. Sturdevant, and Gary Duncan. 2007. "Event-Based Data Collection for Generating Actuated Controller Performance Measures:" Transportation Research Record, January. https://doi.org/10.3141/2035-11.

[11] Montgomery, Douglas, and George Runger. 2018. Applied Statistics and Probability for Engineers. 7th ed. Wiley.

TRAFFIC FLOW THEORY IN ASSESSING DETECTOR PERFORMANCE

Katherine Riffle[1], Edward Smaglik, Ph.D.[2], Steven Proccacio[3], Steven Gehrke, Ph.D.[4], Brendan Russo, Ph.D.[5], and David Hurwitz, Ph.D.[6]

[1, 2, 3, 4, 5] Northern Arizona University

P.O. Box 15600

Flagstaff, AZ 86001

[1]Email: krr264@nau.edu

[2]Email: Edward.Smaglik@nau.edu

[3]Email: slp424@nau.edu

[4]Email: Steven.Gehrke@nau.edu

[5]Email: Brendan.Russo@nau.edu

[6]Oregon State University

101 Kearney Hall,

Corvallis, OR 97331

Email: David.Hurwitz@oregonstate.edu

ABSTRACT

The scope of this study is to develop new methods for evaluating detector health using event-based outputs and existing traffic flow theory. In this work, event-based detector data outputs were used to develop empirical Volume vs. Density curves, per Greenshield's Fundamental Model. Using integration, these empirical lines were compared with a conceptual Volume vs. Density curve for each detector, generated using average headway data and the posted speed limit. Additionally, detector performance and site information were used to model a predicted Volume versus Density relationship for each detector based upon collected data, which was then compared with the Conceptual line in the same manner as the empirical lines. The outcomes of both of these comparisons were then used to create a database to be used for assessing detector health within the structure of an algorithm. The algorithm is then presented and discussed, followed by directions for future research, lessons learned, and limitations of this work.

INTRODUCTION

Past research (Smaglik et al. 2017) has shown declining operational performance from non-invasive detection units at signalized intersections. Specifically, errors in data quality and accuracy showed widespread issues with aging equipment and unmet maintenance needs. Accordingly, there is a need for policies, procedures, and techniques to identify malfunctioning detection equipment and evaluate the quality of data developed by detectors. Current tools,

including those available through the newer Advanced Traffic Controller (ATC) standards, can identify major detector failures in a detector, but cannot assess the quality of the detection outputs. To address this issue, this research applies existing traffic flow theory toward assessing detector health. Event-based detector data outputs are processed to approximate saturated traffic flow, then analyzed according to Greenshield's Model.

LITERATURE REVIEW

The objective of this literature review is to explore previous research relevant to the areas of detector performance, detector health monitoring, and traffic flow theory as it applies to detector operations.

DETECTOR HEALTH MONITORING

The following subsections will detail what is available in scientific as well as vendor literature.

Detector health monitoring with traffic control products and software

Most traffic controllers and detection devices are able to detect major detector failures by examining the presence, absence, or frequency of data being sent by a detector.
One vendor's products, Q-Free/Intelight's MAXTIME local control software, includes three ways to identify a malfunctioning sensor ("MAXVIEW Atms" 2020). Collectively these features are called "detector diagnostics" in the software. These are an optional feature that can be programmed per detector: No Activity – Assume a failure if no calls are received on a detector

for a configurable period of time; Max Presence – Assume a failure if a continuous call is placed on a detector for a configurable period of time; Erratic Count – Assume a failure if more than a specified number of calls are placed on a detector in a configurable period of time. MAXVIEW does identify detector faults, but only at the ends of the performance spectrum. If performance has degraded slightly due to increased latency or some other performance issue, this would likely not be identified.

Other vendors incorporate similar capabilities in their control software. Econolite's Centracs SPM central system specifications notes that this system applies statistical data science to analyze detectors that may not be fully operational, and creates a list within the monitored corridor that may have degraded detector performance (Econolite 2020b). To accomplish this, Econolite's traffic controller can be programmed to identify a lack of activity on a certain detector by time of day as a possible failure. Additionally, their SPM tool can identify differences from recent historical data to flag a failure.

McCain is another manufacturer that sells controllers and intersection control software, but their published literature does not detail how their products address sensor health (McCain 2020), and attempts to acquire further information from the manufacturer were unsuccessful.

Health monitoring in inductive loop and radar detection units consists of primarily reporting faults and logging them. Vendor websites did not detail how faults were identified, however given what is known about common practices, it is presumed that faults are identified by examining the presence, absence, or frequency of data being sent by a detector. (Econolite 2020a; Iteris 2020; Reno A&E 2020; "Wavetronix - SmartSensor V" 2020)

Detector health monitoring through algorithms / post processing

Algorithms can be used either in real time or through post-processing to identify problematic detector operation. Statistical methods can be used to identify outliers, infeasible data, and erroneous data, making it suitable to develop graphs and tables to find the location of the erroneous data within the data set. From there, it is possible to find the detector itself that was causing the poor data quality. While this study is focused on interrupted flow facilities, algorithms applied to uninterrupted flow are considered.

Researchers at the Washington State Transportation Center developed an algorithm to identify and correct dual-loop sensitivity problems that resulted in inaccurate reporting of truck volumes. Using individual vehicle information developed from event based high resolution data, the researchers were able to identify sensitivity discrepancies and then retune the detectors, with the end result of this work being the implementation of the algorithm in a software tool for convenient usage (Nihan, Wang, and Cheevarunothai 2006). In a study that used loop detector data from almost 15,000 Caltrans inductive loops, malfunctioning loops were identified through their volume and occupancy measurements. These measurements were compared against values at neighboring detectors as well as historical data to identify when a detector may be problematic, improving on earlier methods that only relied on data from a single detector (Chen et al. 2003). In related work, researchers at the University of Nebraska developed a methodology to identify malfunctions such as detector and communication failures that lead to erroneous data (Vanajakshi and Rilett 2006). This research focused on the conservation of vehicles principle on

42

a system-wide level to identify locations where the principle was violated. It was then validated using a CORSIM model.

The Portland Oregon Regional Transportation Archive Listing (PORTAL) is the ITS data archive for freeway loop detector data for the Portland metropolitan region, documenting aggregated data and performance measures. Data uploaded into PORTAL is filtered to identify erroneous data through a series of data quality flags as well as comparison against plausibility thresholds. For the former technique, if a detector logs a speed as zero when the same detector logs a count greater than zero, a flag is raised. For the latter technique, data samples that have a speed above 100 miles per hour or below five miles per hour would be flagged. Data samples are then broken into four categories: Good, Suspicious (failed one or more data quality conditions), No Traffic, or Communication Failure. This information is then made known to the user when downloaded and can also be plotted to identify the scale of erroneous data by type of filter (Tufte et al. 2007).

Researchers in Sweden and Finland collaborated to develop a Fuzzy Intelligent Traffic Signal (FITS) control, a method which provides an inexpensive approach to improve signal control based on road infrastructure (J Jin et al. 2016). A simulation-based framework is used to evaluate different traffic control strategies based on certain criteria such as vehicle flows, pedestrian flows, priorities, and platoon management. In this methodology, stop line detectors assist in vehicle actuated timing and advance detectors play a crucial role in the decision making process (J Jin et al. 2016). In running their FITS simulations, the researchers determined that traffic states can still be properly estimated and proper decisions can be made even if a few detectors are malfunctioning, though the authors noted that there is a threshold where this falls apart (J Jin et al. 2016). Another project that related detection performance to advanced signal control was

commissioned by Oregon DOT and completed in 2017 (Smaglik et al., 2017). In this project, researchers at Northern Arizona University led a team that investigated the impact on non-invasive detection performance on adaptive control. As part of their site evaluation, researchers noted that only 42% of the coupled detection zones (inductive loop and non-invasive technology) passed a human ground truth comparison. Additionally, the research team was able to identify other poorly performing detectors by comparing collected detector data (for example, occupancy with a video detector) with expected performance norms. One of the conclusions of this study was that detector health monitoring is critical for sensors used for higher level control.

In a recent study, a screening tool was developed to identify detector errors from data within the Utah DOT detector data database. This work used statistical analysis as well as historical detector information to identify malfunctioning detectors from data within the database through a multi-stage process, using a combination of historical data, data from neighboring detectors, and the application of traffic flow theory to detector data to identify problematic detectors. Data was compiled from UDOT's Performance Measurement System (PeMS) from detectors along a corridor. The PeMS system received vehicle count and occupancy data at 20 second intervals. Speed, flow, and occupancy were analyzed to find potential errors in a one-month data collection period. The primary method of detector health evaluation in this study was through comparison of adjacent detectors upstream or downstream of each other on this roadway. (TRB 2020)

## TRAFFIC FLOW THEORY AND FUNDAMENTAL WORK

Greenshields Model

Traffic flow theory is the basis of conceptual modeling of traffic. Greenshields Model of traffic flow (Greenshields 1935) illustrates the connected nature of volume (V), speed (S), and density

(D) within traffic operations. This relationship, shown in Equation 1, leads to the fundamental

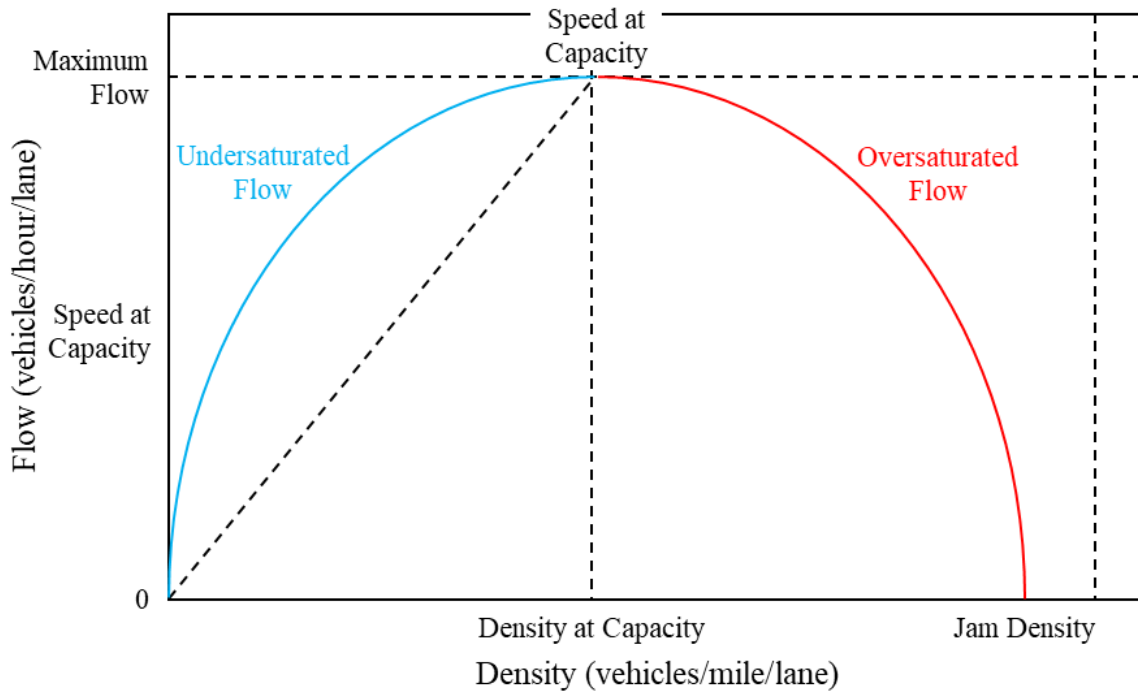diagrams of the Greenshields model, shown in Fig. 8.

$$V = S * D \tag{1}$$
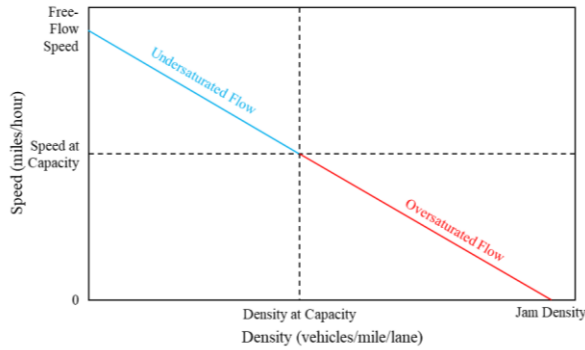
(a) Speed vs Density
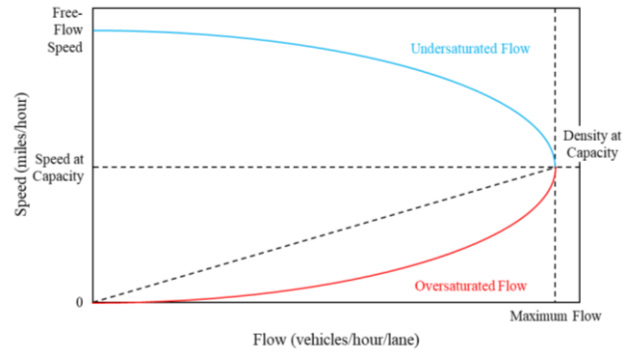
(b) Speed vs Flow (Volume)

(c) Flow (Volume) vs Density

Fig. 8. Fundamental Diagrams of Greenshields Model: (a) Speed vs Density; (b) Speed vs Flow

(Volume); (c) Flow (Volume) vs Density

45

These diagrams illustrate the idealized conceptual relationships between the three macroscopic traffic stream parameters, volume, speed, and density. They encompass two distinct regions of flow, undersaturated (under capacity) and oversaturated (over capacity). These diagrams are conceptual in nature, in that volume, speed, and density data collected to model traffic flow at any given location when plotted would not give way to a smooth diagram as is shown in Fig. 8. The fundamental diagrams have been used in traffic research to assist in the investigation of incident detection (Jing Jin and Ran 2009), car-following models for simulation (Deng and Zhang 2012), the effects of weather on traffic operations (Dhaliwal et al. 2017), and variable speed limits (Bertini, Boice, and Bogenberger 2006), among other topics, but have not been used in detector health applications.

Saturated flow rate and headways

The departing vehicle flow rate at capacity from a signalized intersection is defined as the Saturation Flow Rate. This rate of flow occurs as vehicles in a standing queue depart, starting from the fifth vehicle in the queue as the first four vehicles in the queue depart at a lower flow rate due to time lost as the queue moves from a stopped to a moving queue (Transportation Research Board 2016). It can be directly measured in the field by counting the vehicles departing at capacity during a certain time period. It can also be determined in the field by measuring departure headways of vehicles departing at capacity, with headway defined as, "the time between successive vehicles as they pass a point on a lane or roadway, measured from the same point on each vehicle" (Transportation Research Board 2016). The relation between headway and volume is shown in Equation 2. If the headway measured occurs during queue discharge at capacity, the corresponding volume that will be calculated will be that of the saturation flow rate.

$$V = \frac{3600}{h} \hspace{4cm} (2)$$

The concepts of headway, saturation headway, and saturation flow rate were developed through applied research, and as part of the foundation of traffic operations theory, appear in research endeavors covering all aspects of traffic theory, including intersection capacity (Laufer et al. 2019), the impact of automated vehicles on mixed-use lanes (Mohajerpoor and Ramezani 2019), bicycle operations (Raksuntorn and Khan 2003), geometric design (Potts et al. 2007), and weather conditions (Asamer and Van Zuylen 2011), among others, but they have not been applied to detector health.

LITERATURE REVIEW SUMMARY

This literature review has covered the state of the practice regarding detector health monitoring and the elements of traffic theory that are applied to analyzing detector health in this research. In the area of detector health, three different techniques were covered in this literature review: monitoring with traffic control products and software, monitoring with algorithms / post processing, and on-site monitoring. Finally, Greenshields model and content within the Highway Capacity Manual form the theoretical basis for capacity analysis of interrupted and uninterrupted flow facilities. These methods, along with the fundamental diagrams yielded through application of Greenshields' model, and combined with high resolution detection data, reveal an opportunity to monitor detector health through traffic flow information on a per intersection approach basis. In this study, the Fundamental Diagrams of Greenshields Model, Fig. 8, and the associated theories are used to develop an algorithm for identifying detector malfunctions. The conceptual quadratic relationship between Density and Volume is integral in deriving methods of detector health evaluation. Other relationships derived from the fundamental relationship between

volume, speed, and density, shown in Equation 1, incorporate more aspects of the detector data and the detector's location characteristics into this evaluation. Approximating uninterrupted saturated traffic flow is necessary for analyzing the data using existing traffic theory.

DATA PREPARATION AND VERIFICATION

The initial data collection and processing methods organize and filter the event-based detector outputs for events that best represent uninterrupted traffic flow for each detector. These are explained in the following sections.

EVENT LOG DATA

Event Log data from vetted detection devices at six selected sites were used to develop algorithms for identifying poorly performing detectors. This Event Log Data reported information using Event IDs and corresponding Parameters (Christopher Day et al. 2014). While there are many different types of events contained in a typical log, the list of used Event IDs and the corresponding Parameter used in this task are shown in TABLE 1. Event IDs 1 and 8 were used to identify the start of each green and yellow phase, with timestamps attached to specific events used to determine the length of each cycle and each green and yellow/red phase. Event IDs 82 and 81 indicated the Vehicle Detector On and Vehicle Detector Off, respectively. With all radar and loop detection zones operating in presence, data from these events were used to determine activations (which are used as a surrogate for vehicle counts in this work, as count detector outputs are not available) and occupancy, which was used to evaluate the efficacy of the detection zones at the study sites.

TABLE 1. Event Log IDs and Parameters (Christopher Day et al. 2014)

Event ID	Name	Description	Parameter Description
1	Phase Begin Green	Set when either solid or flashing green indication has begun	Phase #
8	Phase Begin Yellow Clearance	Set when phase yellow indication becomes active and clearance timer begins	Phase #
81	Vehicle Detector Off	Vehicle detector has turned off. Detector on and off events are triggered post any detector delay/extension processing	Vehicle Detector #
82	Vehicle Detector On	Vehicle detector has turned on. Detector on and off events are triggered post any detector delay/extension processing	Vehicle Detector #

Two of the sites used for this work were equipped with radar detection, in addition to inductive loop detection. At the outset of the analysis, it was determined that only radar count zones operating in 'Normal' mode (which is akin to a loop detector operating in presence mode) would be used in this analysis, as the outputs of the larger stop line and advance radar detection zones are manipulated by proprietary vendor software to achieve various objectives, and as such cannot be linked to traffic theory. Thus, they are excluded from analysis. TABLE 2 lists the number of days of data available for each site.

TABLE 2. Event Log Data Availability for Each of Six Intersections

Intersection	Dates	Days Available
OR22 @ I-5SB Ramp	8/2/20 – 8/8/20; 10/5/20 – 2/15/21	133
OR34 @ I-5	8/2/20 – 8/8/20; 10/5/20 – 2/15/21	140
OR34 @ Peoria	8/2/20 – 8/8/20; 10/5/20 – 2/15/21	133
US20 @ 15th	8/14/20 – 8/17/20; 10/5/20 – 2/15/21	137
US26 @ Meinig	8/26/20; 10/5/20 – 2/15/21	134
US101@ 22nd	8/2/20 – 8/8/20; 10/5/20 – 2/15/21	133

DATA CLEANSING AND PREPARATION

Cleansing raw data for processing

Approximately 19 weeks of raw data was provided for each of the six intersections, each with multiple detection zones (45 in total). It should be noted that each detection zone used in this work had been assessed with a performance heuristic from prior research. Data from the sufficiently performing detectors were then used to build the relationships and algorithms documented in the subsequent sections.

The raw data were first filtered for small errors that would impede the evaluation. There are two known issues with the provided event-based data, that of repeated 'Detector On' events for the same detector, and that of repeated 'Green On' interval data events. Repeating indications for Vehicle Detector On and Vehicle Detector Off were removed to ensure data consistency, while cycles where repeating indications for Green Time Start and Yellow Time Start occurred were removed to ensure that green durations and their related volume characteristics were consistent from cycle to cycle.

Data preparation

A number of additional filtering techniques were applied to remove variability in the data analyzed, and provide the most consistent data sets for analysis of detector health. First, given that approximation of saturated uninterrupted flow would require high volumes, the data from peak commuting periods (Tuesday, Wednesday, and Thursday, from 6:00 AM – 9:00 AM and 4:00 PM – 7:00 PM) were used for analysis.

Second, due to the start-up lost time as described in the literature review, the first four vehicles

of each cycle would need to be removed from the analysis as they exhibit headways which are

larger than the headways during saturated flow (Transportation Research Board 2016). Finally,

as the goal was to model saturated flow, activations with headways above a certain threshold

were removed from the analysis.

Regarding headways, the reported average headways are between 2.96 and 3.01 for vehicles

traveling in corridors with speed limit ranges reflected in these study intersections

(Transportation Research Board 2016). To determine the cutoff for removing vehicles with

larger headways, headways were evaluated per vehicle position in the queue for each green-

phase interval. The plot in Fig. 9 represents three hours of afternoon peak period headway data

for one detector, sorted by vehicle position. As can be seen in the figure, the median headway for

each vehicle position is roughly between 2.5s and 4.0s. with additional data points logged well

above the median for most vehicle positions.
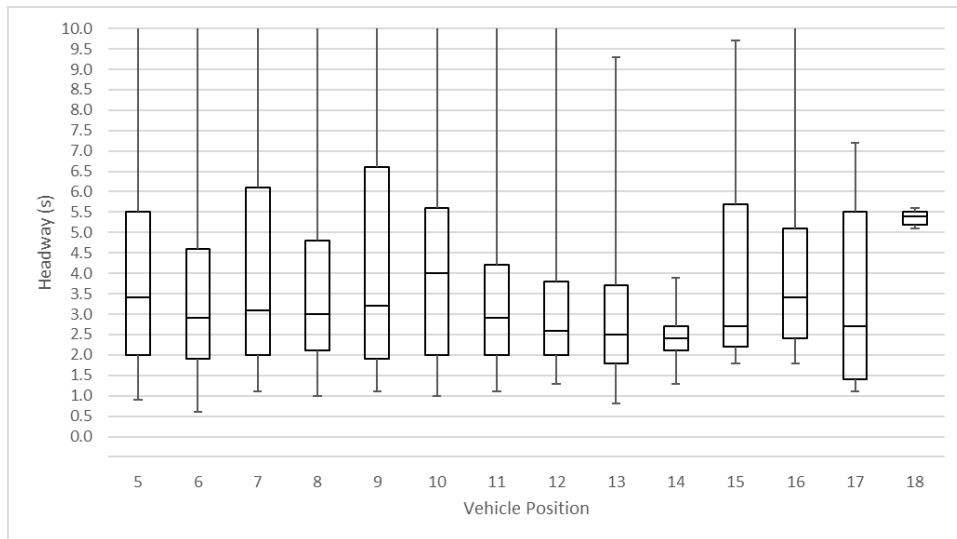
Fig. 9. Headway Data per Vehicle Position, No Data Removed, for One Detector

The first step taken toward filtering out headways not representative of uninterrupted traffic flow

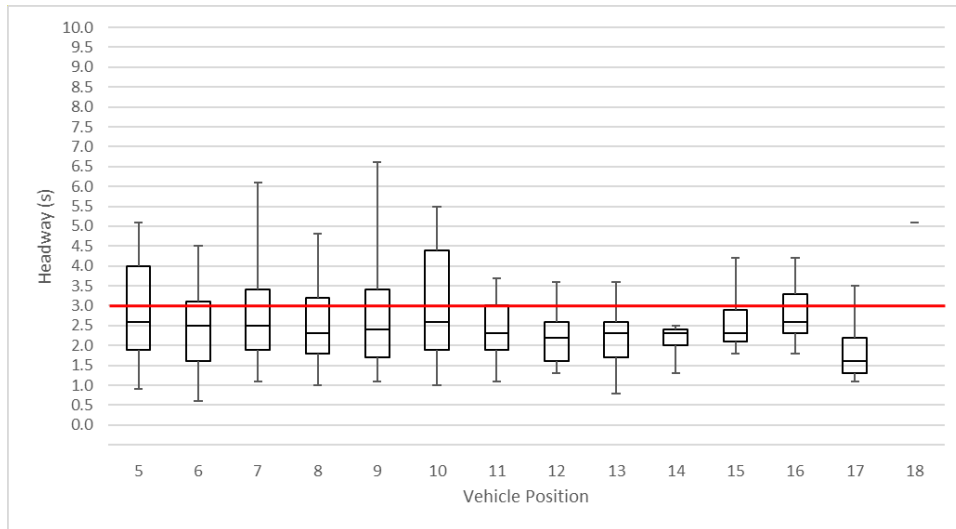was removing the top quartile of headways for each position, as shown in Fig. 10.

Fig. 10. Headway Data per Vehicle Position, Top Quartile of Headway Data Removed from Each Vehicle

Position, for One Detector

While this succeeded in removing some of the larger headways, the resulting data still contained

many headways that were not indicative of saturated flow. Several other approaches were

applied to limit the number of headways in the data that would represent non-saturated flow,

including removing headways larger than two or three times the median headway for each

position, removing activations that are detected within the last 6.0 seconds before the yellow-

phase interval, and removing the data from the entire green-phase interval if the first vehicle's

headway was greater than 8.0 seconds. In the end, it was determined that limiting the headways

used in this work to 3.0 seconds, a common value used in setting gap timers within actuated

control, would more effectively accomplish the desired outcome without the need to carry out

complicated mathematical procedures. Reducing the number of complicated mathematical

procedures was necessary for developing a more communicable algorithm that could be

interpreted into a coding language; moreover, the results of these procedures supported that the cutoff headway should be 3.0s, a value supported by existing traffic theory (Transportation Research Board 2016). This approach has the added benefit of including activations later in the green interval as part of the data analysis, as saturated conditions can occur well into stale green. The red line in Fig. 10 indicates the 3.0 second cutoff for headway data. Note that the median headway value for each vehicle position is below this line, indicating that the majority of headways are captured by this method.

DATA ANALYSIS

The purpose of the data analysis was to evaluate detector health using existing traffic flow theories and variables. Raw data outputs from the detector were processed and used to determine the detector health.

EMPIRICAL LINE DEVELOPMENT: EHV AND DENSITY

After the raw data had been cleansed and prepared, the Equivalent Hourly Volume (EHV) and Density were calculated for each detector on a cycle basis. Equation 3 shows the calculation for EHV, using the number of activations during green as a surrogate for departure volume. It was noted that several vehicles may arrive on red, and these were not captured in departure volume.

$$EHV = {3600}/{(3600 \times 24 \times C)}(A) \tag{3}$$

Equation 4 shows the calculation for density, using occupancy per green interval as a surrogate. Both of these metrics were calculated on an individual cycle basis.

$$D = \frac{O \times 5280}{(L_{Veh} + L_{Det})} \tag{4}$$

$$Occupancy = Detector\ On\ Duration \div Cycle\ Duration \tag{5}$$

For density, the vehicle length was assumed to be the design passenger vehicle length of 19 feet

(*A Policy on Geometric Design of Highways and Streets* 2011), while Detector Length was

provided as measurements from the field (or approximated in the case of radar detection zones).

A constant vehicle length was used in this process with precedent in typical traffic analyses. A

different vehicle length could be selected, and while it would impact the resulting calculations,

the impact would be consistent across all data processed, as this value is a constant.

Once the processing was completed for an entire week of data (Tuesday, Wednesday, and

Thursday from 6:00 AM – 9:00 AM and 4:00 PM – 7:00 PM), the dataset was plotted and an

empirical line of best fit was created by applying a quadratic best fit line to the plotted data, as

shown in Fig. 11. The figure also shows the Coefficient of Determination (R^2) for the fit of the

line to the data, as well as a conceptual Volume vs. Density line derived from site information

for that detector.
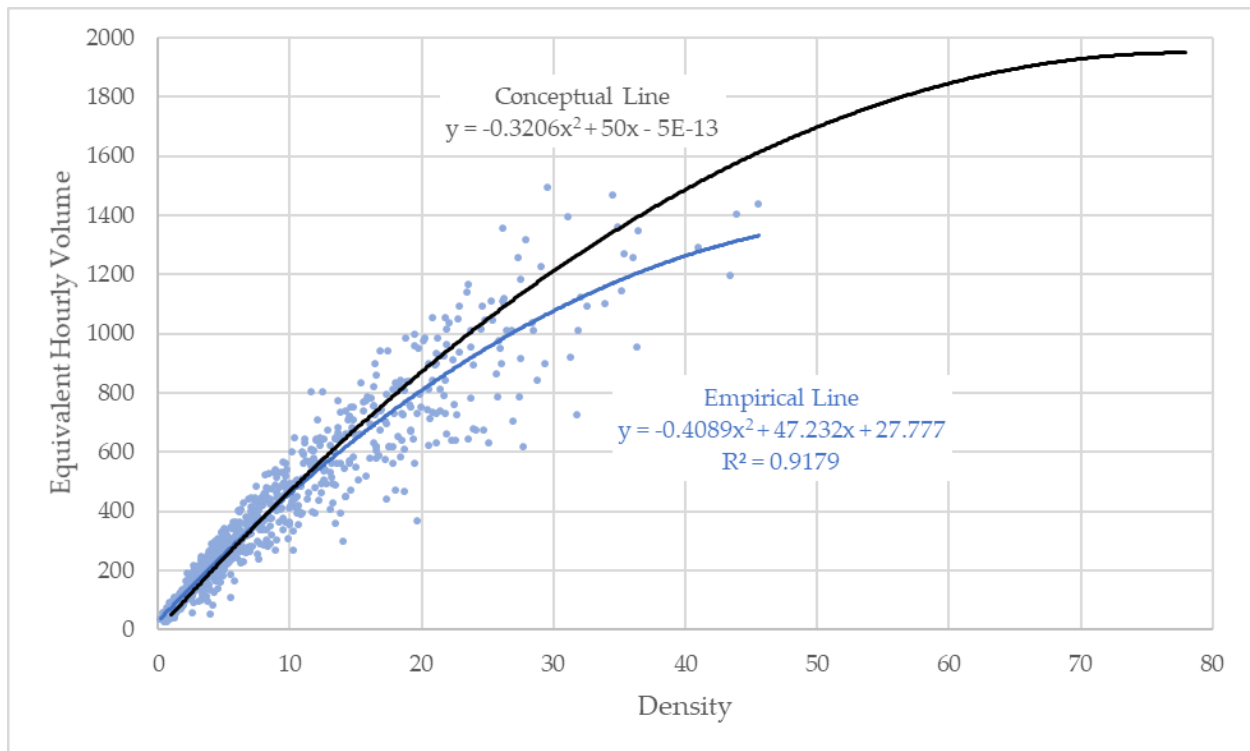
Fig. 11. Example Empirical Line and Empirical Data, and Conceptual Line

For weeks of data with fewer than 50 data points, an empirical line was not developed due to

data insufficiency; detectors with fewer than 50 data points per week had less reliable data

because the vehicle activations were more irregular and did not represent the typical, largely

undersaturated state of the detector. Additionally, any empirical line with an R^2 less than 0.70

was not used for further analysis, as an R^2 less than 0.7 generally indicates a weak or moderate

fit (Montgomery and Runger 2018).

Lastly, outlier control was performed to improve the correlation between EHV and Density, and

reduce variability in the processed data. The interquartile range method was applied to remove

data points located at the ends of the spectrum of plotted data. In this method, the interquartile

range (IQR) (i.e. the 75th percentile – the 25th percentile of the data set) is calculated, and any

point falling below the 25th percentile – 1.5*IQR or above the 75th percentile + 1.5*IQR is

removed as an outlier. Applying this method reduced both the mean and standard deviation of the processed data., as well as reduced the standard deviation, indicating a reduction in the variability of the data set. As such, both EHV and Density outliers identified with this method were removed.

CONCEPTUAL LINE DEVELOPMENT

The conceptual quadratic relationship was developed for each detector using the Optimum Density (Equation 6) and Maximum Equivalent Hourly Volume (Equation 7), per Greenshield's relationship (Equation 1), using an average headway for the detector and the speed limit of the approach.

$$D_O = \frac{V_{Max}}{S_O} \tag{6}$$

$$V_{Max} = \frac{3600}{Average\ Headway} \tag{7}$$

While the Optimum Speed was determined to be ½ the posted speed limit, an approximation directly derived from Greenshield's work, several sets of data for a detector were analyzed to determine the most effective method of calculating the average headway. TABLE 3 shows the average headway for a detector for various days and time periods of analysis. Given the relatively small spread in the average headway from the various windows of data analyzed, and the fact the event-based data is collected at a 0.1s resolution, it was determined that using the average headway for the first day of data would be sufficient.

TABLE 3. Average Headways for Sensitivity Analysis

Date	Average Headway (seconds)
Jan 12	2.11
Jan 12-14	2.08
Jan 19-21	2.08
Feb 2-4	2.06
Jan 12-14, Jan 19-21	2.08
Jan 12-14, Jan 19-21, and Feb 2-4	2.07

PREDICTED LINE DEVELOPMENT

After establishing a quadratic relationship between vehicle volume and density in development

of a site-specific conceptual line, the method for assessing detector health at these locations was

advanced by modeling the empirical data set to produce detector-specific predicted lines for

comparison. The choice of an appropriate modeling technique for predicting these empirical

lines, however, was contingent on having sufficient data observed at each location, these data

exhibiting a downward parabolic shape when fit to a quadratic curve, additional site-level data

available to explore how independent factors may contribute to observed volume-density curve

variation, and a model structure that accounts for the interdependence between observed a, b,

and c terms in the quadratic formula in predicting empirical lines at each location. The form of a

quadratic expression is shown in Equation 8.

$$y = ax^2 + bx + c \tag{8}$$

An initial step in the modeling process was the construction of a data set with sufficient

representation at each location across the four weeks of collected data. Accordingly, a potentially

complete sample of 180 records (four weeks of empirical data collected at 45 locations) was

reduced to a sample of 106 records after removing records with empirical data fewer than ten

points (74 records). Of this remaining sample, five records were removed in which the a term

57

exhibited a positive value, which would have produced an upward parabolic shape when plotted, resulting in a final sample of 101 records.

Using the reduced sample, a next analytic step was to specify multiple regression models where observed values of a, b, and c were functions of various site characteristics that may account for variation in these outcome variables. Given the inter-relationship between the three outcome variables and a desire to model a single set of predictor variables, a multivariate multiple regression modeling structure was chosen. Specification of predictors in this simultaneous model of multiple outcomes was pursued with an iterative process that first assessed statistically significant intergroup (or model outcome) differences in the effects of independent predictors and then examined the explanatory power of any selected predictor variables. Regarding the former assessment, a multiple analysis of variance (MANOVA) was conducted to test differences in mean values of a, b, and c terms per location across several categorical site characteristics. TABLE 4 summarizes the results of this analysis in which significant variation was found for mean values of the a, b, or c terms in each of the tested categorical variables except for detector length. Of note, continuous measures of green activation and detector indication were examined as binary variables in the MANOVA, with low and high values based on relationship of locational measure with mean value of variables within the full final sample.

	a				*b*				*c*			
	Mean	SD	Min	Max	Mean	SD	Min	Max	Mean	SD	Min	Max
Study sample (n=101) *	-0.333	0.396	-2.876	-0.003	31.589	15.799	0.440	76.858	24.411	31.875	-43.426	182.680
Week 1 (n=25)	-0.391	0.580	-2.876	-0.003	32.773	15.300	1.572	60.183	18.129	33.676	-43.426	151.920
Week 2 (n=25)	-0.290	0.280	-1.203	-0.003	31.249	14.761	1.838	60.204	24.368	33.496	-4.092	168.150
Week 3 (n=26)	-0.282	0.232	-0.964	-0.005	30.074	14.492	2.447	55.122	28.731	36.060	0.192	182.680
Week 4 (n=25)	-0.370	0.417	-1.838	-0.003	32.322	19.095	0.440	76.858	26.243	23.622	-2.049	110.320
Study sample (n=101) *	-0.333	0.396	-2.876	-0.003	31.589	15.799	0.440	76.858	24.411	31.875	-43.426	182.680
0: Tech Loop (n=21)	0.108	0.150	-0.581	-0.006	20.941	8.520	7.723	48.414	19.510	12.389	-0.568	47.687
1: Tech Loop (n=80)	-0.392	0.420	-2.876	-0.003	34.385	16.109	0.440	76.858	25.697	35.202	-43.426	182.680
Study sample (n=101) *	-0.333	0.396	-2.876	-0.003	31.589	15.799	0.440	76.858	24.411	31.875	-43.426	182.680
0: Detect Advance (n=44)	-0.157	0.300	-1.838	-0.003	21.384	9.031	0.440	48.414	18.654	22.296	-20.946	110.300
1: Detect Advance (n=57)	-0.468	0.410	-2.876	-0.003	39.467	15.430	1.572	76.858	28.855	37.235	-43.426	182.680
Study sample (n=101) *	-0.333	0.396	-2.876	-0.003	31.589	15.799	0.440	76.858	24.411	31.875	-43.426	182.680
0: Main Street (n=29)	-0.246	0.526	-2.876	-0.003	21.538	11.337	1.572	53.939	31.962	51.714	-43.426	182.680
1: Main Street (n=72)	-0.367	0.328	-1.838	-0.003	35.638	15.587	0.440	76.858	21.369	18.539	-4.092	110.320
Study sample (n=101) *	-0.333	0.396	-2.876	-0.003	31.589	15.799	0.440	76.858	24.411	31.875	-43.426	182.680
0: Single Lane (n=16)	-0.350	0.212	-0.821	-0.053	43.523	17.286	15.130	76.858	34.750	21.327	-20.946	77.010
1: Single Lane (n=85)	-0.329	0.423	-2.876	-0.003	29.343	14.545	0.440	60.204	22.465	33.228	-43.426	182.680
Study sample (n=101) *	-0.333	0.396	-2.876	-0.003	31.589	15.799	0.440	76.858	24.411	31.875	-43.426	182.680
0: > 10-ft Length (n=66)	-0.358	0.421	-2.876	-0.003	31.313	15.011	1.572	60.204	24.173	34.942	-43.426	182.680
1: > 10-ft Length (n=35)	-0.284	0.344	-1.838	-0.003	32.111	17.403	0.440	76.858	24.859	25.569	-20.946	110.320
Study sample (n=101) *	-0.333	0.396	-2.876	-0.003	31.589	15.799	0.440	76.858	24.411	31.875	-43.426	182.680
0: Thru Lane Only (n=34)	-0.26	0.49	-2.88	0.00	21.40	11.38	0.44	53.94	29.67	48.83	-43.43	182.68
1: Thru Lane Only (n=67)	-0.37	0.34	-1.84	0.00	36.76	15.26	2.14	76.86	21.74	18.05	-4.09	110.32
Study sample (n=101) *	-0.333	0.396	-2.876	-0.003	31.589	15.799	0.440	76.858	24.411	31.875	-43.426	182.680
0: High Activation (n=61) ^	-0.232	0.440	-2.876	-0.003	22.304	10.298	0.440	53.939	25.475	38.839	-43.426	182.680
1: High Activation (n=40) ^	-0.486	0.254	-1.203	-0.020	45.750	11.675	15.714	76.858	22.788	16.732	-4.092	50.243
Study sample (n=101) *	-0.333	0.396	-2.876	-0.003	31.589	15.799	0.440	76.858	24.411	31.875	-43.426	182.680
0: High Indication (n=56) ^	-0.431	0.324	-1.838	-0.053	39.609	13.711	15.130	76.858	19.696	18.306	-20.946	77.013
1: High Indication (n=45) ^	-0.210	0.445	-2.876	-0.003	21.609	12.188	0.440	53.939	30.279	42.740	-43.426	182.680

Notes:

* Reduction of complete sample (n=180) after removing records with non-negative value for *a* (n=72) or less than 10 observations (n=74).

^ High represents activation/indication level above the mean value for the study sample ($\bar{x}$ activations = 304.927 and $\bar{x}$ indications = 37.476).

Cells in GREEN reflect a statistically significant difference in group means (p<0.05).

Cells in BLUE reflect a marginally significant difference in group means (p<0.10).

Having established that significant mean differences across the outcomes existed for seven independent variables, a backwards elimination model specification process was undertaken to determine a consistent set of predictors in the multivariate multiple regression model used to create the predicted empirical line. The final model specification—shown in TABLE 5—was determined once the removal of a single predictor resulted in no improvement to the adjusted R^2 value of the reduced model and that the Type II MANOVA test statistic for each remaining predictor variable was marginally statistically significant (p<0.10). Looking at individual model performances, the overall fit for the model of the *b* term (R^2=0.661) was higher than the

specification for the a term (R^2=0.172) and c term (R^2=0.154). The presence of advanced

detection technology and the continuous green activation metric were statistically significant in

each specification, with these two variables being the lone significant predictors in the b term

model. The former predictor as well as the presence of a loop detector were only marginally

significant in the a term model, while the number of indications, presence of advanced detector

technology, and site location within a single lane roadway were all statistically significant

($p<0.05$) in the c term model.

TABLE 5. Multivariate Multiple Regression Model Estimates

Predictor Variable	*a*			*b*			*c*		
	Beta	Std. Error	p-value	Beta	Std. Error	p-value	Beta	Std. Error	p-value
(intercept)	0.629	0.338	0.066	6.337	8.624	0.464	-10.341	27.478	0.707
Tech Loop	-0.267	0.136	0.052	3.773	3.472	0.280	9.171	11.062	0.409
Detect Advance	-0.180	0.100	0.074	6.754	2.542	0.009	21.385	8.098	0.010
Single Lane	-0.171	0.120	0.157	4.700	3.062	0.128	-29.725	9.758	0.003
Activations	-0.001	<0.001	0.022	0.064	0.007	<0.001	-0.047	0.024	0.051
Indications	-0.008	0.006	0.162	-0.136	0.145	0.348	1.458	0.461	0.002
Model Summary									
Adjusted R^2			0.172			0.661			0.154

Using this final multivariate multiple regression model specification, the final step was to predict

the value of a, b, and c terms for each combination of detector location and week of empirical

data. Prediction of a maximum of four empirical lines per detector location was accomplished by

inserting the observed value of each predictor variable in the final model specification for all

records. While predictive estimates for a, b, and c terms using every week of recorded detector

data helps to provide a more robust assessment of detector health, a location-level aggregation of

these terms across the data collection period can also be useful in investigating the predictive

model's performance at sites with varying characteristics not isolated in the final specification.

COMPARING CONCEPTUAL, PREDICTED, AND

EMPIRICAL LINES

The concept of mathematical integration was used for comparing the performance of the

conceptual Volume/Density curve with predicted and empirical approximations of that curve.

Then, the percent difference in the integral value between two curves was compared and used as

a metric for analysis.

For each individual detector, two different percent difference calculations were made. First, a

percent difference calculation was made between each respective weekly empirical line.

Equation 9 shows the calculation for the percent difference between the integral values between

weeks.

$$\boldsymbol{Percent\ Difference = 100 \times \frac{(week\ n+1)-(week\ n)}{(week\ n)}} \tag{9}$$

Because four weeks of data were processed for each detector, a total of six percent differences

were generated, as each week was treated as an individual data point, regardless of the temporal

sequence of the data: Week 2 compared to Week 1, Week 3 compared to Week 1, Week 4

compared to Week 1, Week 3 compared to Week 2, Week 4 compared to Week 2, and Week 4

compared to Week 3.

Given the typical application of field data to an uninterrupted conceptual Volume/Density

diagram, initial integration bounds for these comparisons were 0 and the x-coordinate of the

vertex of the conceptual curve (100% vertex as shown in Fig. 12). However, because the majority

of the plotted data points fell within 0 to 50% of the x-axis vertex range, comparative integrals

were developed for four different sets of ranges, from 0% to 100% of the x-axis vertex

coordinate, in 25% increments. Four complete weeks of data were able to be collected from 25 of

the verified detectors. These datasets developed the metrics shown in TABLE 6 and Fig. 13 for determining the appropriate integration bounds for the percent difference calculations. Fig. 12 shows an example detector's data to illustrate the empirical line, predicted line, and conceptual line being integrated to specific bounds.
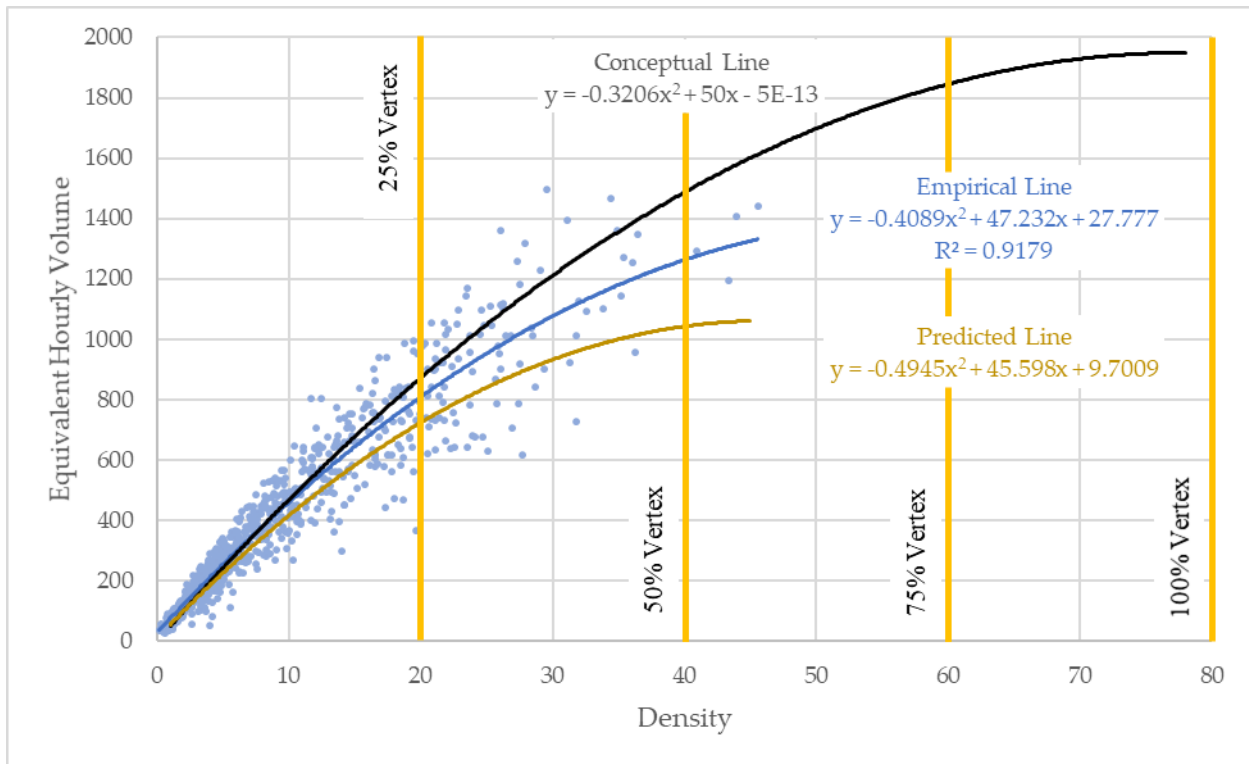

Fig. 12. Empirical Line, Predicted Line, and Conceptual Curve with Integration Bounds (25%, 50%, 75%, and 100% of the Conceptual Curve)

Four complete weeks of data were able to be collected from 25 of the verified detectors; some detectors did not have four complete weeks of data. Overall, 578 percent difference data points developed the summary data shown in Fig. 13 which was used for determining the appropriate integration bounds for the percent difference calculations. Fig. 13 shows the cumulative percent differences for each integration bound. A line is drawn at the 20% difference bin to allow for a comparison between the four trace lines. This line illustrates that, at this point on the plot,

roughly 80% of the data points in both the 25% and 50% threshold have values of 20% percent difference or lower; only 70% of the data is encompassed for the 75% threshold, and 65% for the 100% threshold. More data points below 20% are an indicator of less week to week variability.
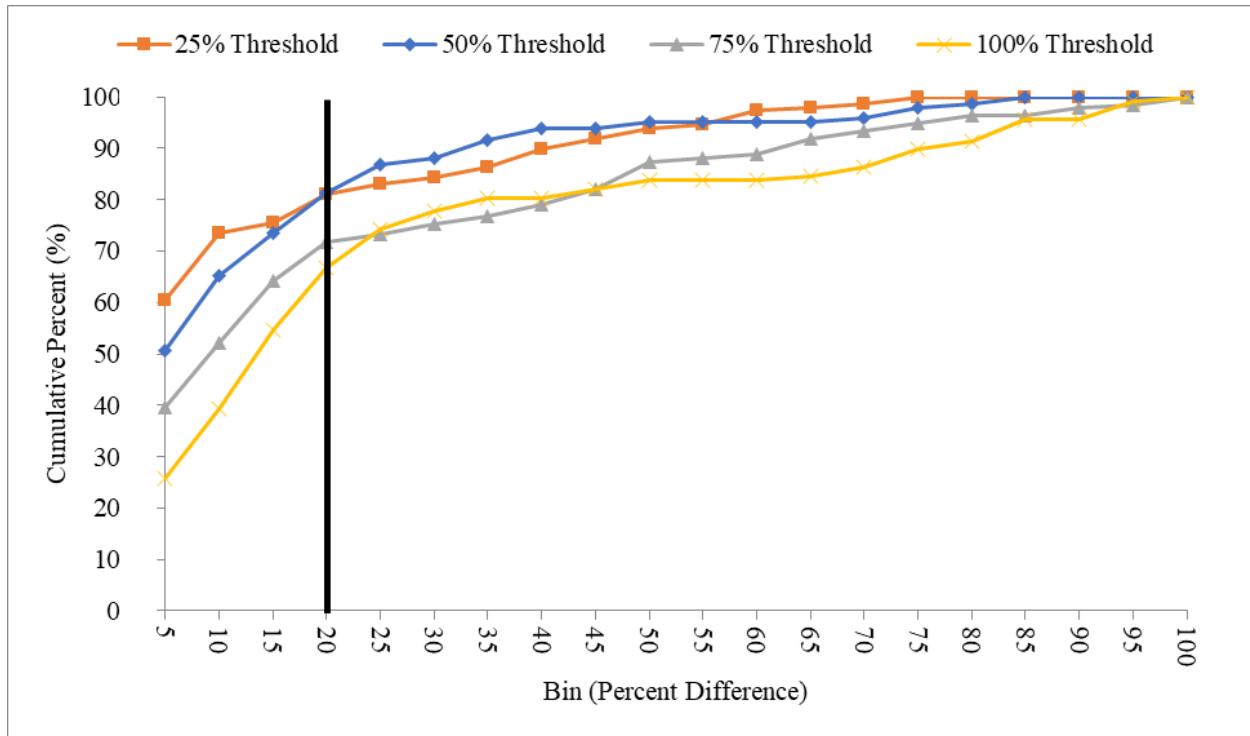
Fig. 13. Cumulative Percent Difference Comparison of the Integration Thresholds

The percent differences when integrated to 100% of the conceptual vertex were typically the highest, as can be seen in TABLE 6, which summarizes the mean and standard deviations of each of the distributions. Both the mean and standard deviation continued decrease as the integration bounds were reduced, with the smallest values observed at the 25% threshold.

TABLE 6. Mean and Standard Deviation of Integration Values at Different Integration Thresholds

	25%	50%	75%	100%
Mean	10.64	13.51	24.54	142.55
Std Dev	16.69	24.81	36.36	386.77

Because of this, the desire to have roughly 80% of the percent difference values at or below 20% (black line shown in Fig. 13), and the fact that the majority of data points developed to create the empirical lines were in this section of the plots, it was determined that using bounds of 0 to 25% of the theoretical vertex would provide the most predicable performance assessment, as the mean and standard deviation will be used in the detector health analysis.

Next, a percent difference calculation was made between the conceptual line for each detector and the predicted line for each week for that respective detector (predicted line shown in Fig. 12), integrating from 0 to 25% of the conceptual vertex. The distribution of these percent differences is shown in Fig. 14; the mean of this data is 2.8 percent difference and the standard deviation is 5.5 percent difference.
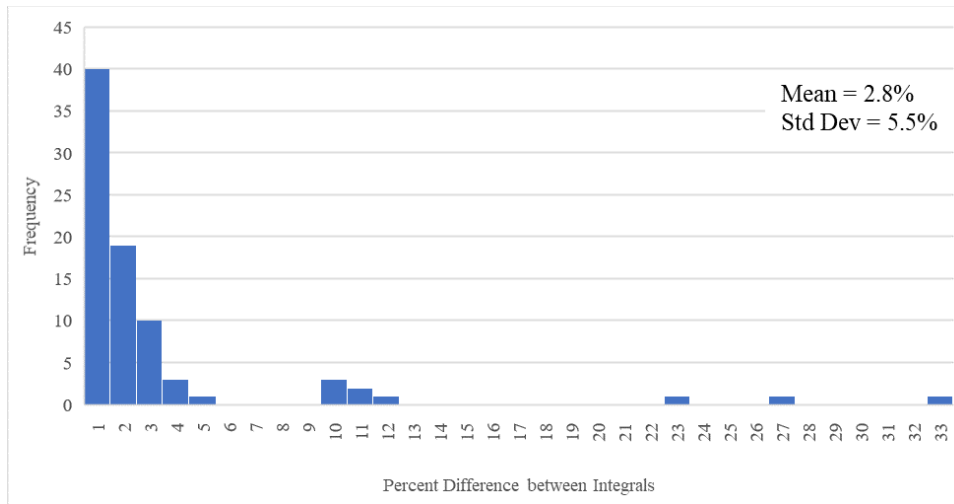
Fig. 14. Percent Difference between Conceptual and Predicted Line Integrals for All Detectors

The data in Fig. 14 is representative of all of the sufficient detectors in the developed performance dataset. The mean and standard deviation were then used as a baseline for the detector health algorithm; the mean for the detector being evaluated should fall within 1.5 standard deviations of that mean. The percent differences between the integrals of each detector

being evaluated are compared to the mean and standard deviation of the developed performance

dataset percent differences as described in the following algorithm.

ALGORITHM FOR INITIAL HEALTH ASSESSMENT

The general form of this health assessment is illustrated in Fig. 15. It shows the process for using

the data outputs from the detectors and the site characteristics to model three types of lines for

use in the detector health assessment. A Predicted Volume versus Density curve and a

Conceptual Volume versus Density curve were derived and compared as a metric for detector

health upon initial implementation of this algorithm. The variations in the Empirical Volume

versus Density data was analyzed over four weeks of data to assess the detector's health over

time.
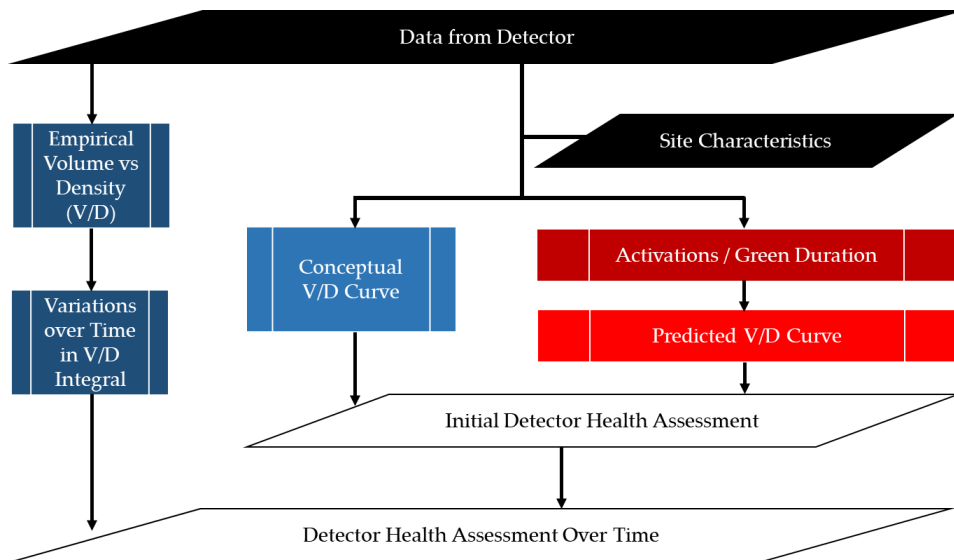
Fig. 15. Data Analysis Flowchart

The algorithm describes how processed data from the detector and site characteristics from the

detector's location are used to derive an assessment of the detector's functional status. It uses the

detector's derived conceptual line, the predicted line derived from the first week of data, and the best fit empirical lines from the first four weeks of data. The algorithm for assessing detector health upon initial implementation is shown in Fig. 16. The process for each step is discussed in the successive text.
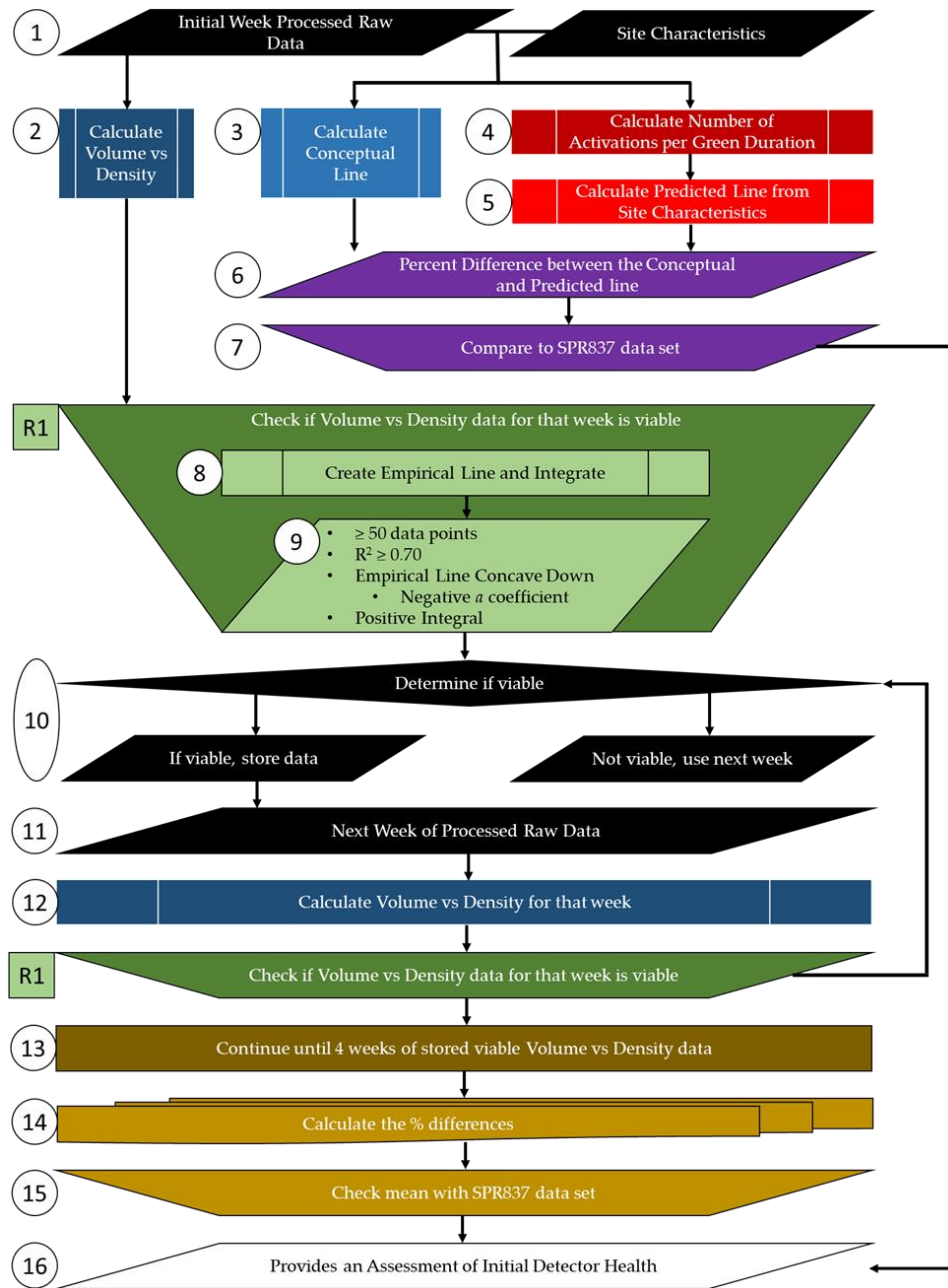

Fig. 16. Initial Health Assessment Flowchart

1) <u>Input: Initial Week of Processed Raw Data</u>. One week of cleansed data is used in the algorithm for the Initial Health Assessment. <u>Input: Site Characteristics</u>. The site characteristics include the movement's speed limit, which is used in the process of calculating the conceptual line, as well as aspects of the detector's location used to model the predicted line.

2) <u>Process: Calculate Volume vs Density</u>. The raw data are processed and the volume versus density relationships in the empirical data are derived.

3) <u>Process: Calculate Conceptual Line</u>. The conceptual line is calculated.

4) <u>Process: Calculate Number of Activations per Green Duration</u>. The raw data are processed and the number of activations per green-phase as well as the green-phase duration is found for each cycle.

5) <u>Process: Calculate Predicted Line from Site Characteristics</u>. Site characteristics, activation data, and existing output models are used to calculate the predicted line.

6) <u>Output: Percent Difference between Conceptual and Predicted Lines</u>. The determined Conceptual and Predicted lines are compared by finding the percent differences between their integrals.

7) <u>Compare to the developed performance dataset</u>. The percent difference between the conceptual and predicted lines' integrals is compared against the sufficient detectors' dataset (25% column in TABLE 6).

8) <u>(Routine 1) Processes: Check if Volume vs Density for that week is viable</u>. First an empirical line is best fit to the initial week of volume vs density data.

9) <u>(Routine 1) Output</u>: There are multiple checks for this data and its empirical line. The data set for the initial week must have 50 or more data points; the *Coefficient of Determination* (R^2) for the empirical line fit to the data set must be greater than or equal to 0.70; the empirical line must be concave down; and the empirical line must have a positive integral when integrated from 0 to 25% of the Conceptual line's vertex. These checks determine if the initial week of empirical data is viable for assessing the detector's health.

10) <u>Decision: Determine if viable</u>. The checks described above determine if the initial week of data is viable for this assessment. If it is not viable, the following week of data should be instead analyzed in these processes to see if it is viable. If the initial week of data is viable, then the empirical line's integral from 0 to 25% of the conceptual line's vertex should be stored.

11) <u>Input</u>: The next week of processed raw data is now used in the algorithm for the initial health assessment.

12) <u>Process</u>: The volume vs density data should be analyzed for this next week.

<u>(Routine 1)</u> Determine if the volume vs density for that week is viable, similarly to how it was determined for the initial week, creating an empirical line and integrating it as part of the process. The same bounds are used for integration as were for the first week of data.

13) <u>Process</u>: If this data is viable, the integral is stored, and the process moves onto the next week of processed data. This algorithm continues until there are 4 weeks of viable data.

14) <u>Multiple Data Sets</u>: The 4 weeks of empirical line integrals are compared by their percent differences. Six data points of percent difference between integrals result from this comparison.

15) <u>Compare to developed performance data set.</u> The mean of the percent differences between the empirical lines over four weeks is compared to the developed performance dataset (mean in TABLE 6).

16) <u>Output</u>: The percent differences calculated above must be within 1.5 standard deviations of the developed performance data set mean (noted in steps 7 and 15). If one or both are outside this value, it is an indicator of possible poor detector health.

CONCLUSIONS

In this work, event-based detector data were processed for a variety of detectors at select signalized intersections to first identify which detectors were performing sufficiently to be used for development of an algorithm. Event-based detector data outputs were analyzed according to Greenshields Models, providing guidance for post-processing data analysis techniques. Each detector's average headway data for one week was used to derive a Conceptual line for that detector, incorporating the posted speed limit at that location. Site detector performance information was modeled to predict a Volume versus Density relationship, which was compared with the Conceptual line and related to a database developed in this work for an estimate of initial health. Four weeks of empirical data were also compared with a separate a developed performance dataset within this work. A value more than 1.5 standard deviations from the mean of the developed performance dataset was proposed as a starting point for health assessment, but this may be adjusted for sensitivity in identifying underperforming detectors.

Moving forward, as noted in the paragraph above, it would be advisable to investigate different bounds for the sensitivity analysis. Commonly used bounds were applied, which may not be the most suitable for vehicle detector health monitoring. Additionally, as this algorithm is implemented, it is advised to develop percent difference datasets for detectors of various technologies and configurations so that comparisons can be made between field detectors and datasets developed from detectors with similar characteristics. This can be done by segregating percent difference data from various detectors as additional sites are brought online. This should allow for tighter control limits for determining sensor health, as variation in the comparative data set would be limited by the homogenous categorization of detectors.

Limitations include that the developed algorithm and datasets are modeled from a finite number of detectors. As such, the datasets developed for health assessment are based upon this set of analyzed detectors, which may not be a universally representative sample of detectors. Based upon comparisons between the healthy and unhealthy detector datasets in this work, the methods proposed will identify a variety of unhealthy detector operations, however the thresholds chosen can be tightened up with further testing.

ACKNOWLEDGEMENTS AND DISCLAIMER

NOTATION LIST

The following symbols are used in this paper:

A	=	Number of Activations per Green Duration
C	=	Cycle Duration
D	=	Density (vehicles/mile)
D_O	=	Optimum Density
EHV	=	Equivalent Hourly Volume
L_{Det}	=	Detector Length
L_{Veh}	=	Average Vehicle Length
O	=	Occupancy
S	=	Speed (miles/hour)
S_O	=	Optimum Speed (½ of Posted Speed Limit)
V	=	Volume (vehicles/hour)
V_{Max}	=	Maximum Volume
h	=	Departure headway (seconds/vehicle)

REFERENCES

A Policy on Geometric Design of Highways and Streets. 2011. 6th ed. American Association of
State Highway and Transportation Officials.

Arnold, J, D Gibson, M Mills, M Scott, and J Youtcheff. 2011. "Using GPR to Unearth Sensor
Malfunctions." *Federal Highway Administration* 74 (4): pp 24-29.

Asamer, Johannes, and Henk J. Van Zuylen. 2011. "Saturation Flow under Adverse Weather
Conditions." *Transportation Research Record* 2258 (1): 103–9. https://doi.org/10.3141/2258-
13.

Bertini, Robert L., Steven Boice, and Klaus Bogenberger. 2006. "Dynamics of Variable Speed
Limit System Surrounding Bottleneck on German Autobahn." *Transportation Research
Record* 1978 (1): 149–59. https://doi.org/10.1177/0361198106197800119.

Chen, C, J Kwon, J Rice, A Skabardonis, and P Varaiya. 2003. "Detecting Errors and Imputing
Missing Data for Single Loop Surveillance Systems." In , 25 p. Washington DC, United
States.

Day, Thomas Brennan, Jr., James Sturdevant, and Darcy Bullock. 2011. "Performance
Evaluation of Traffic Sensing and Control Devices." FHWA/IN/JTRP-2011/17. Purdue
University. https://doi.org/10.5703/1288284314641.

Day, C, H Premachandra, T Brennan Jr., J Sturdevant, and D Bullock. 2010. "Operational
Evaluation of Wireless Magnetometer Vehicle Detectors at Signalized Intersection."
Transportation Research Board, no. 2192: pp 11-23.

Day, Christopher, Darcy Bullock, Howell Li, Steve Remias, Alexander Hainen, Richard Freije,
Amanda Stevens, James Sturdevant, and Thomas Brennan. 2014. "Performance Measures for

Traffic Signal Systems: An Outcome-Oriented Approach." *JTRP Affiliated Reports*, August. https://doi.org/10.5703/1288284315333.

Day, Christopher, H Premachandra, T Brennan Jr., J Sturdevant, and D Bullock. 2010. "Operational Evaluation of Wireless Magnetometer Vehicle Detectors at Signalized Intersection." *Transportation Research Board*, no. 2192: pp 11-23. https://doi.org/10.3141/2192-02.

Deng, Hui, and H. Michael Zhang. 2012. "Driver Anticipation in Car Following." *Transportation Research Record* 2316 (1): 31–37. https://doi.org/10.3141/2316-04.

Dhaliwal, Sawanpreet Singh, Xinkai Wu, John Thai, and Xudong Jia. 2017. "Effects of Rain on Freeway Traffic in Southern California." *Transportation Research Record* 2616 (1): 69–80. https://doi.org/10.3141/2616-08.

Econolite. 2020a. "AccuSense Control - Econolite Radar Vehicle Detection." *Econolite* (blog). 2020. https://www.econolite.com/products/detection/accusense-control/.

———. 2020b. "Centracs SPM Specifications." May 2020. https://www.econolite.com/wp-content/uploads/specifications/systems-centracsspm-specification.docx.

Greenshields, B.D. 1935. "A Study in Highway Capacity." *Highway Research Board Proceedings* 14: 448–77.

Grossman, Jay, Alexander M. Hainen, Stephen M. Remias, and Darcy M. Bullock. 2012. "Evaluation of Thermal Image Video Sensors for Stop Bar Detection at Signalized Intersections." *Transportation Research Record* 2308 (1): 184–98. https://doi.org/10.3141/2308-20.

Hill, John D., and Linda Ng Boyle. 2007. "Driver Stress as Influenced by Driving Maneuvers

and Roadway Conditions." *Transportation Research Part F: Traffic Psychology and*

Behaviour 10 (3): 177–86. https://doi.org/10.1016/j.trf.2006.09.002.

Huotari, John. 2015. "City Moving to Radar-Based Systems to Detect Vehicles at Stoplights."

December 11, 2015. https://oakridgetoday.com/wp-content/uploads/2015/12/Stoplight-

Radar-Detection-Dec-11-2015.jpg.

Hurwitz, David S., Michael A. Knodler, Bruce Nyquist, Derek Moore, and Halston Tuss. 2012.

"Evaluating the Potential of Advanced Vehicle Detection Systems in Mitigating Dilemma

Zone Safety Conflicts." *ITE Journal* 82 (3). https://trid.trb.org/view/1135967.

INDOT. 2015. "Procedure for Evaluating Vehicle Detection Performance." Government.

Indiana.Gov. 2015. https://www.in.gov/indot/div/mt/itm/pubs/934_testing.pdf.

Iteris. 2020. "Iteris Vantage Vector." May 2020. https://www.iteris.com/products/detection-

sensors/vantage-vector-hybrid.

Jin, J, X Ma, K Koskinen, M Rychlik, and I Kosonen. 2016. "Evaluation of Fuzzy Intelligent

Traffic Signal Control (FITS) System Using Traffic Simulation." In , 11 p. Washington DC,

United States: Transportation Research Board.

Jin, Jing, and Bin Ran. 2009. "Automatic Freeway Incident Detection Based on Fundamental

Diagrams of Traffic Flow." *Transportation Research Record* 2099 (1): 65–75.

https://doi.org/10.3141/2099-08.

Kuhnel, C, T Weisheit, and R Hoyer. 2011. "Malfunction Sniffing – A New Approach for On-

Site Quality Evaluations of Traffic Data Acquisition Infrastructure." In , 7p. Orlando Florida,

United States: Intelligent Transportation Systems.

Kyte, Michael, Zaher Khatib, Patrick Shannon, and Fred Kitchener. 2001. "Effect of Weather on
Free-Flow Speed." *Transportation Research Record* 1776 (1). https://doi.org/10.3141/1776-
08.

Lamas, Jose, Paula-Maria Castro-Castro, Adriana Dapena, and Francisco Vazquez-Araujo. 2016.
"SiDIVS: Simple Detection of Inductive Vehicle Signatures with a Multiplex Resonant
Sensor." *Sensors* 16 (August): 1309. https://doi.org/10.3390/s16081309.

Laufer, Julian, Wen Long Yue, Zahra Shahhoseini, and Farid Javanshour. 2019. "Determination
of Saturation Flows in Melbourne," 8.

Marnell, Patrick. 2020. "ODOT Research - Portland Oregon, Sensors and Controllers," May 18,
2020.

"MAXVIEW Atms." 2020. Q-Free | Intelight. 2020. https://www.intelight-
its.com/products/intelight-maxview-atms/.

McCain. 2020. "Traffic Signal Controllers & Modules | McCain." 2020. https://www.mccain-
inc.com/products/controllers.

Medina, Juan C., Hani Ramezani, and Rahim (Ray) F. Benekohal. 2013. "Evaluation of
Microwave Radar Vehicle Detectors at a Signalized Intersection under Adverse Weather
Conditions." *Transportation Research Record* 2366 (1): 100–108.
https://doi.org/10.3141/2356-12.

Middleton, Dan, Hassan Charara, and Ryan Longmire. 2009. "Alternative Vehicle Detection
Technologies for Traffic Signal Systems: Technical Report." Technical Report Report 0-
5845-1. https://static.tti.tamu.edu/tti.tamu.edu/documents/0-5845-1.pdf.

Middleton, Dan, Ryan Longmire, Darcy M. Bullock, and James R. Sturdevant. 2009. "Proposed Concept for Specifying Vehicle Detection Performance." *Transportation Research Record* 2128 (1): 161–72. https://doi.org/10.3141/2128-17.

Minge, Erik, Jerry Kotzenmacher, and Scott Peterson. 2010. "Evaluation of Non-Intrusive Technologies for Traffic Detection." Final Report MN/RC 2010-36. Minnesota Department of Transportation. https://www.lrrb.org/pdf/201036.pdf.

Mohajerpoor, Reza, and Mohsen Ramezani. 2019. "Mixed Flow of Autonomous and Human-Driven Vehicles: Analytical Headway Modeling and Optimal Lane Management." *Transportation Research Part C: Emerging Technologies* 109 (December): 194–210. https://doi.org/10.1016/j.trc.2019.10.009.

Montgomery, Douglas, and George Runger. 2018. *Applied Statistics and Probability for Engineers*. 7th ed. Wiley.

Nihan, N, Y Wang, and P Cheevarunothai. 2006. "Improving Dual-Loop Truck (and Speed) Data: Quick Detection of Malfunctioning Loops and Calculation of Required Adjustments." *National Transportation Library*, 63 p.

Potts, Ingrid B., John F. Ringert, Karin M. Bauer, John D. Zegeer, Douglas W. Harwood, and David K. Gilmore. 2007. "Relationship of Lane Width to Saturation Flow Rate on Urban and Suburban Signalized Intersection Approaches." *Transportation Research Record* 2027 (1): 45–51. https://doi.org/10.3141/2027-06.

Raksuntorn, Winai, and Sarosh I. Khan. 2003. "Saturation Flow Rate, Start-Up Lost Time, and Capacity for Bicycles at Signalized Intersections." *Transportation Research Record* 1852 (1): 105–13. https://doi.org/10.3141/1852-14.

Reno A&E. 2020. "Reno A&E Vehicle Detectors." May 2020.

    http://www.renoae.com/Category/root/30.

Rhodes, Avery, Darcy Bullock, and James Sturdevant. 2006. "Evaluation of Stop Bar Video

    Detection Accuracy at Signalized Intersections." Final Report FHWA/IN/JTRP-2005/28,

    2869. West Lafayette, IN: Purdue University. https://doi.org/10.5703/1288284313401.

Sharma, Anuj, Matthew Harding, Brad Giles, Darcy M Bullock, James R Sturdevant, and

    Srinivas Peeta. 2008. "Performance Requirements and Evaluation Procedures for Advance

    Wide Area Detectors." *Transportation Research Board*, 26.

Smaglik, Edward J., Anuj Sharma, Darcy M. Bullock, James R. Sturdevant, and Gary Duncan.

    2007. "Event-Based Data Collection for Generating Actuated Controller Performance

    Measures:" *Transportation Research Record*, January. https://doi.org/10.3141/2035-11.

Smaglik, C Sobie, A Sharma, C Liu, and S Kothuri. 2017. "Improving Adaptive/Responsive

    Signal Control Performance: Implications of Non-Invasive Detection and Legacy Timing

    Practices." Final Report FHWA-OR-RD-17-07. Oregon.

Transportation Research Board. 2016. *Highway Capacity Manual 6th Edition: A Guide for*

    Multimodal Mobility Analysis. https://doi.org/10.17226/24798.

TRB. 2020. "Multi-Stage Algorithm for Detection-Error Identification and Data Screening."

    May 28, 2020. https://rip.trb.org/view/1602146.

Tufte, K, S Ahn, R Bertini, B Auffray, and J Rucker. 2007. "Toward Systematic Improvement of

    Data Quality in Portland, Oregon, Regional Transportation Archive Listing." In , 11 p.

    Washington DC, United States: Transportation Research Board.

Usman, Taimur, Liping Fu, and Luis F. Miranda-Moreno. 2010. "Quantifying Safety Benefit of
Winter Road Maintenance: Accident Frequency Modeling." *Accident Analysis & Prevention*
42 (6): 1878–87. https://doi.org/10.1016/j.aap.2010.05.008.

Vanajakshi, L, and L Rilett. 2006. "System-Wide Data Quality Control of Inductive Loop Data
Using Nonlinear Optimization." *Journal of Computing in Civil Engineering* 20 (3): pp 187-
196.

Wang, Haizhong, Jia Li, Qian-Yong Chen, and Daiheng Ni. 2011. "Logistic Modeling of the
Equilibrium Speed–Density Relationship." *Transportation Research Part A: Policy and
Practice* 45 (6): 554–66. https://doi.org/10.1016/j.tra.2011.03.010.

"Wavetronix - SmartSensor V." 2020. 2020. https://www.wavetronix.com/products/en/6.

LIST OF TABLES

LIST OF FIGURES

4.0   OVERALL DISCUSSION OF RESULTS AND

CONCLUSIONS

In this thesis, event-based detector data were processed for a collection of detectors at signalized intersections in Oregon. To first identify which detectors were performing sufficiently to be foundational in an algorithm development, a manual detector health check was performed: For the six study sites in this work, Event Log data provided by ODOT personnel was compared with manually compiled detector data developed using a novel collection technique, that of drone video, to determine suitability of the existing detectors to be used in further research. This study developed and tested a new method of detector health evaluation by statistically comparing manually collected and transcribed drone video data to event-based detector output logs. A total of 79 detection zones underwent the above comparative analysis (70 inductive loop and 9 radar). The radar detection zones were not compared through Detector On Duration, only through Number of Activations, to the drone videos. Of the inductive loop detection zones, 39 passed the analysis, while 6 of the radar zones passed the analysis, for a total of 45 valid detection zones, ~60% of the total analyzed. This study was limited by the amount of video footage possible to take, the variety in signalized intersection detectors provided, and the small sample of radar detectors. The subset of detection zones that passed the comparative analysis included stop line, advanced, single lane, multiple lane, short, and long detection zones over a variety of lane usages and provided a robust basis for the successive research.

The algorithm developed from the validated detectors' datasets and from fundamental traffic theory evaluated detector health through multiple analyses. Events occurring Tuesday through

Thursday during the morning and evening peak period were filtered to be considered the dataset for one week of data. Additional information was collected from each detector, including its lane of travel, the lane width, the detector length, and the posted speed limit for that road segment. For one week of data for each detector, the datasets were further filtered to remove repeats in the Detector On, Detector Off, Green Phase Start, and Yellow Phase Start events, and any corresponding data that may be affected by these repeats. The datasets were then processed to obtain the Number of Activations per Green Interval, and each Green Interval Duration, for one week of data. The same datasets were further filtered to better approximate uninterrupted flow: vehicles were removed from the datasets to account for start-up lost time, and vehicles with large headways were removed from consideration to account for gaps in the traffic flow. From the resulting datasets, the detector's Equivalent Hourly Volume and Density were derived for each cycle. These data were plotted and a quadratic line of best fit, the Empirical line, was used to describe the Equivalent Hourly Volume and Density relationship for one week of data. The viability of each week of Equivalent Hourly Volume and Density data was checked using the line of best fit's *Coefficient of Determination*, the number of data points available for the dataset, that the Empirical line was concaved down and that its integral was positive. For insufficient datasets, the following week of data was used instead.

Each detector's average headway data for one week were used to derive a Conceptual line for that detector, incorporating the posted speed limit at that location. The Conceptual line was used to compare to the initial week's Empirical line for an initial health assessment. The comparison between these lines was done by calculating the integral for each line from 0 to 25% of the Conceptual line's vertex – the Maximum Volume – and finding the percent difference between

these integration values. Four weeks of Empirical data was used for the initial detector health assessment; the mean of the percent differences between the Conceptual line and each week's Empirical line is compared to the mean and standard deviation of the percent differences found in the previously developed performance datasets.

Once a complete Empirical Volume versus Density dataset was created for each of the sufficiently-performing detectors in the dataset, this information was used to create a model for a predicted Volume versus Density relationship. This model incorporated the Number of Activation data from each week and additional characteristics from the detector's site to create a Predicted line for each detector per week. The Predicted line for each detector's first week of data and the Conceptual line for the detector were compared as another metric for initial detector health, similarly to how the Conceptual and the Empirical lines were compared. Four weeks of Empirical data was used for the initial detector health assessment. This algorithm provides guidance for the action and implementation of detector health analysis as a low-cost option for updating faulty infrastructure.

The limitations of this study and developed algorithm include that they were modeled based off of the datasets from a finite number of detectors. In the model created from the developed performance dataset, not every detector configuration was addressed, due to the small sample of detectors. The sensitivity testing provided another limitation for this study and developed algorithm: the increase and decrease in Volume and Density data for sensitivity testing of the algorithm were incremented by 10%, 20%, and 30%; these percent increases and decreases were chosen arbitrarily. Another limitation of the project was that it was not feasible to provide long-

term testing of the detector health assessment over time. It is predicted that after one year of data

is collected for the detector's health assessment over time, the detector will have its own dataset

to compare to rather than comparing to this limited developed performance dataset. Also, due to

time constraints, the algorithm developed in this work was not subjected to long term testing and

validation. Based upon comparisons between the healthy and unhealthy detector datasets in this

work, the methods proposed will identify a variety of unhealthy detector operations, however the

thresholds chosen can be tightened up with further testing.

In this study and algorithm development, the pseudocode was derived from a process undertaken

in *Microsoft Excel*. This *Excel Macros* in this program were used to process the datasets and

derive the relationships between Volume and Density. The scope of this project was not to create

a working code, but the limited processing power of *Microsoft Excel* was not ideal for managing

big datasets. A more elegant solution to processing this data using code or other programs would

improve the processing time and reduce the number of mistakes, as well as increase the amount

of data that could be processed simultaneously.

Moving forward, it would be advisable to investigate different bounds for control chart limits

(presumably statistically based). Because existing literature provided no guidance for applying

this method to detector data, commonly used bounds were applied, which may not be the most

suitable for vehicle detector health monitoring. Additionally, as this algorithm is implemented, it

is advised to develop percent difference datasets for detectors of various technologies and

configurations so that comparisons can be made between field detectors and datasets developed

from detectors with similar characteristics. This can be done by segregating percent difference data from various detectors as additional sites are brought online. This should allow for tighter control limits for determining sensor health, as variation in the comparative data set would be limited by the homogenous categorization of detectors.

This thesis contributes to the existing literature and detector health monitoring methods by introducing a new process of manually verifying vehicle detectors and developing a new algorithm towards automated detector monitoring. The new verification process based on drone video collection is useful for deriving very accurate performance data from detectors at intersections without cameras. This process would be primarily useful for collecting research data. The developed algorithm from this study improves the efficiency of widespread detector malfunction monitoring for individual detectors at signalized intersections, without reliance on in-person evaluations. To continue developing this algorithm, further research into the long-term health analysis of individual detectors is suggested. Implementation into existing systems, such as ones at state DOTs, would most successfully utilize this algorithm for detector monitoring.

5.0   REFERENCES

A Policy on Geometric Design of Highways and Streets. 2011. 6th ed. American Association of
State Highway and Transportation Officials.

Arnold, J, D Gibson, M Mills, M Scott, and J Youtcheff. 2011. "Using GPR to Unearth Sensor
Malfunctions." *Federal Highway Administration* 74 (4): pp 24-29.

Asamer, Johannes, and Henk J. Van Zuylen. 2011. "Saturation Flow under Adverse Weather
Conditions." *Transportation Research Record* 2258 (1): 103–9.
https://doi.org/10.3141/2258-13.

Bertini, Robert L., Steven Boice, and Klaus Bogenberger. 2006. "Dynamics of Variable Speed
Limit System Surrounding Bottleneck on German Autobahn." *Transportation Research
Record* 1978 (1): 149–59. https://doi.org/10.1177/0361198106197800119.

Chen, C, J Kwon, J Rice, A Skabardonis, and P Varaiya. 2003. "Detecting Errors and Imputing
Missing Data for Single Loop Surveillance Systems." In , 25 p. Washington DC, United
States.

Day, Thomas Brennan, Jr., James Sturdevant, and Darcy Bullock. 2011. "Performance
Evaluation of Traffic Sensing and Control Devices." FHWA/IN/JTRP-2011/17. Purdue
University. https://doi.org/10.5703/1288284314641.

Day, C, H Premachandra, T Brennan Jr., J Sturdevant, and D Bullock. 2010. "Operational
Evaluation of Wireless Magnetometer Vehicle Detectors at Signalized Intersection."
Transportation Research Board, no. 2192: pp 11-23.

Day, Christopher, Darcy Bullock, Howell Li, Steve Remias, Alexander Hainen, Richard Freije,
Amanda Stevens, James Sturdevant, and Thomas Brennan. 2014. "Performance Measures
for Traffic Signal Systems: An Outcome-Oriented Approach." *JTRP Affiliated Reports*,
August. https://doi.org/10.5703/1288284315333.

Day, Christopher, H Premachandra, T Brennan Jr., J Sturdevant, and D Bullock. 2010.
"Operational Evaluation of Wireless Magnetometer Vehicle Detectors at Signalized
Intersection." *Transportation Research Board*, no. 2192: pp 11-23.
https://doi.org/10.3141/2192-02.

Deng, Hui, and H. Michael Zhang. 2012. "Driver Anticipation in Car Following."
Transportation Research Record 2316 (1): 31–37. https://doi.org/10.3141/2316-04.

Dhaliwal, Sawanpreet Singh, Xinkai Wu, John Thai, and Xudong Jia. 2017. "Effects of Rain on Freeway Traffic in Southern California." *Transportation Research Record* 2616 (1): 69–80. https://doi.org/10.3141/2616-08.

Econolite. 2020a. "AccuSense Control - Econolite Radar Vehicle Detection." *Econolite* (blog). 2020. https://www.econolite.com/products/detection/accusense-control/.
———. 2020b. "Centracs SPM Specifications." May 2020. https://www.econolite.com/wp-content/uploads/specifications/systems-centracsspm-specification.docx.

Greenshields, B.D. 1935. "A Study in Highway Capacity." *Highway Research Board Proceedings* 14: 448–77.

Grossman, Jay, Alexander M. Hainen, Stephen M. Remias, and Darcy M. Bullock. 2012. "Evaluation of Thermal Image Video Sensors for Stop Bar Detection at Signalized Intersections." *Transportation Research Record* 2308 (1): 184–98. https://doi.org/10.3141/2308-20.

Hill, John D., and Linda Ng Boyle. 2007. "Driver Stress as Influenced by Driving Maneuvers and Roadway Conditions." *Transportation Research Part F: Traffic Psychology and Behaviour* 10 (3): 177–86. https://doi.org/10.1016/j.trf.2006.09.002.

Huotari, John. 2015. "City Moving to Radar-Based Systems to Detect Vehicles at Stoplights." December 11, 2015. https://oakridgetoday.com/wp-content/uploads/2015/12/Stoplight-Radar-Detection-Dec-11-2015.jpg.

Hurwitz, David S., Michael A. Knodler, Bruce Nyquist, Derek Moore, and Halston Tuss. 2012. "Evaluating the Potential of Advanced Vehicle Detection Systems in Mitigating Dilemma Zone Safety Conflicts." *ITE Journal* 82 (3). https://trid.trb.org/view/1135967.

INDOT. 2015. "Procedure for Evaluating Vehicle Detection Performance." Government. Indiana.Gov. 2015. https://www.in.gov/indot/div/mt/itm/pubs/934_testing.pdf.

Iteris. 2020. "Iteris Vantage Vector." May 2020. https://www.iteris.com/products/detection-sensors/vantage-vector-hybrid.

Jin, J, X Ma, K Koskinen, M Rychlik, and I Kosonen. 2016. "Evaluation of Fuzzy Intelligent Traffic Signal Control (FITS) System Using Traffic Simulation." In , 11 p. Washington DC, United States: Transportation Research Board.

Jin, Jing, and Bin Ran. 2009. "Automatic Freeway Incident Detection Based on Fundamental Diagrams of Traffic Flow." *Transportation Research Record* 2099 (1): 65–75. https://doi.org/10.3141/2099-08.

Kuhnel, C, T Weisheit, and R Hoyer. 2011. "Malfunction Sniffing – A New Approach for On-Site Quality Evaluations of Traffic Data Acquisition Infrastructure." In , 7p. Orlando Florida, United States: Intelligent Transportation Systems.

Kyte, Michael, Zaher Khatib, Patrick Shannon, and Fred Kitchener. 2001. "Effect of Weather on Free-Flow Speed." *Transportation Research Record* 1776 (1). https://doi.org/10.3141/1776-08.

Lamas, Jose, Paula-Maria Castro-Castro, Adriana Dapena, and Francisco Vazquez-Araujo. 2016. "SiDIVS: Simple Detection of Inductive Vehicle Signatures with a Multiplex Resonant Sensor." *Sensors* 16 (August): 1309. https://doi.org/10.3390/s16081309.

Laufer, Julian, Wen Long Yue, Zahra Shahhoseini, and Farid Javanshour. 2019. "Determination of Saturation Flows in Melbourne," 8.

Marnell, Patrick. 2020. "ODOT Research - Portland Oregon, Sensors and Controllers," May 18, 2020.

"MAXVIEW Atms." 2020. Q-Free | Intelight. 2020. https://www.intelight-its.com/products/intelight-maxview-atms/.

McCain. 2020. "Traffic Signal Controllers & Modules | McCain." 2020. https://www.mccain-inc.com/products/controllers.

Medina, Juan C., Hani Ramezani, and Rahim (Ray) F. Benekohal. 2013. "Evaluation of Microwave Radar Vehicle Detectors at a Signalized Intersection under Adverse Weather Conditions." *Transportation Research Record* 2366 (1): 100–108. https://doi.org/10.3141/2356-12.

Middleton, Dan, Hassan Charara, and Ryan Longmire. 2009. "Alternative Vehicle Detection Technologies for Traffic Signal Systems: Technical Report." Technical Report Report 0-5845-1. https://static.tti.tamu.edu/tti.tamu.edu/documents/0-5845-1.pdf.

Middleton, Dan, Ryan Longmire, Darcy M. Bullock, and James R. Sturdevant. 2009. "Proposed Concept for Specifying Vehicle Detection Performance." *Transportation Research Record* 2128 (1): 161–72. https://doi.org/10.3141/2128-17.

Minge, Erik, Jerry Kotzenmacher, and Scott Peterson. 2010. "Evaluation of Non-Intrusive Technologies for Traffic Detection." Final Report MN/RC 2010-36. Minnesota Department of Transportation. https://www.lrrb.org/pdf/201036.pdf.

Mohajerpoor, Reza, and Mohsen Ramezani. 2019. "Mixed Flow of Autonomous and Human-Driven Vehicles: Analytical Headway Modeling and Optimal Lane Management." *Transportation Research Part C: Emerging Technologies* 109 (December): 194–210. https://doi.org/10.1016/j.trc.2019.10.009.

Montgomery, Douglas, and George Runger. 2018. *Applied Statistics and Probability for Engineers*. 7th ed. Wiley.

Nihan, N, Y Wang, and P Cheevarunothai. 2006. "Improving Dual-Loop Truck (and Speed) Data: Quick Detection of Malfunctioning Loops and Calculation of Required Adjustments." *National Transportation Library*, 63 p.

Potts, Ingrid B., John F. Ringert, Karin M. Bauer, John D. Zegeer, Douglas W. Harwood, and David K. Gilmore. 2007. "Relationship of Lane Width to Saturation Flow Rate on Urban and Suburban Signalized Intersection Approaches." *Transportation Research Record* 2027 (1): 45–51. https://doi.org/10.3141/2027-06.

Raksuntorn, Winai, and Sarosh I. Khan. 2003. "Saturation Flow Rate, Start-Up Lost Time, and Capacity for Bicycles at Signalized Intersections." *Transportation Research Record* 1852 (1): 105–13. https://doi.org/10.3141/1852-14.

Reno A&E. 2020. "Reno A&E Vehicle Detectors." May 2020. http://www.renoae.com/Category/root/30.

Rhodes, Avery, Darcy Bullock, and James Sturdevant. 2006. "Evaluation of Stop Bar Video Detection Accuracy at Signalized Intersections." Final Report FHWA/IN/JTRP-2005/28, 2869. West Lafayette, IN: Purdue University. https://doi.org/10.5703/1288284313401.

Sharma, Anuj, Matthew Harding, Brad Giles, Darcy M Bullock, James R Sturdevant, and Srinivas Peeta. 2008. "Performance Requirements and Evaluation Procedures for Advance Wide Area Detectors." *Transportation Research Board*, 26.

Smaglik, Edward J., Anuj Sharma, Darcy M. Bullock, James R. Sturdevant, and Gary Duncan. 2007. "Event-Based Data Collection for Generating Actuated Controller Performance Measures:" *Transportation Research Record*, January. https://doi.org/10.3141/2035-11.

Smaglik, C Sobie, A Sharma, C Liu, and S Kothuri. 2017. "Improving Adaptive/Responsive Signal Control Performance: Implications of Non-Invasive Detection and Legacy Timing Practices." Final Report FHWA-OR-RD-17-07. Oregon.

Transportation Research Board. 2016. Highway Capacity Manual 6th Edition: A Guide for Multimodal Mobility Analysis. https://doi.org/10.17226/24798.

TRB. 2020. "Multi-Stage Algorithm for Detection-Error Identification and Data Screening." May 28, 2020. https://rip.trb.org/view/1602146.

Tufte, K, S Ahn, R Bertini, B Auffray, and J Rucker. 2007. "Toward Systematic Improvement of Data Quality in Portland, Oregon, Regional Transportation Archive Listing." In , 11 p. Washington DC, United States: Transportation Research Board.

Usman, Taimur, Liping Fu, and Luis F. Miranda-Moreno. 2010. "Quantifying Safety Benefit of Winter Road Maintenance: Accident Frequency Modeling." *Accident Analysis & Prevention* 42 (6): 1878–87. https://doi.org/10.1016/j.aap.2010.05.008.

Vanajakshi, L, and L Rilett. 2006. "System-Wide Data Quality Control of Inductive Loop Data Using Nonlinear Optimization." *Journal of Computing in Civil Engineering* 20 (3): pp 187-196.

Wang, Haizhong, Jia Li, Qian-Yong Chen, and Daiheng Ni. 2011. "Logistic Modeling of the Equilibrium Speed–Density Relationship." *Transportation Research Part A: Policy and Practice* 45 (6): 554–66. https://doi.org/10.1016/j.tra.2011.03.010.

"Wavetronix - SmartSensor V." 2020. 2020. https://www.wavetronix.com/products/en/6.